EUROPEAN ORGANIZATION FOR NUCLEAR RESEARCH

CERN - PS DIVISION

CERN/PS 94-30 (LP)
CLIC Note 240

BUNCH COMPRESSOR FOR THE CLIC TEST FACILITY

F. Chautard, L. Rinolfi

Abstract

The main goal of the CLIC Test Facility (CTF) is to study the generation of a drive beam with high charge in short bunches. One of the limitations is the space charge effect at low energy which were experimentally verified. In order to balance this effect, it is proposed to produce the requested high charges with a long pulse length, accelerate them and shorten the pulses at the desired value when the energy is high enough.

This note describes the design of a magnetic bunch compressor. The main objective is to produce bunches in the range of 10 nC with a σ_t below 3 ps at the output of the bunch compressor. An optics is also implemented in order to get the beam performances in the CLIC transfer structure. A recall of the theory is given before presenting the results of the beam dynamic simulations.

Geneva, Switzerland
23/8/94

Contents

List of Figures

List of Tables

1 Introduction

For the CLIC machine, the nominal accelerating gradient is 80 MV/m. In order to generate such an electric field at 30 GHz, it would be necessary to produce a single bunch of 54 nC with σ_t = 3 ps crossing the RF CLIC structure [1]. Since such a high charge in a single short bunch would be rather difficult to produce and transport, a proposal [2] using a train of 16 bunches has been made. It corresponds to 7 nC/bunch with the same bunch length σ_z = 1 mm.

Experiments done in the 1993 CTF run [3] are the following (for single bunch):

Laser pulse length: σ_t = 3.5 ps
e^- pulse length at CLIC structure: σ_t = 5.5 ps
Maximum charge at the gun exit: q= 14 nC
Maximum charge at the CLIC structure: q= 7 nC

Experiments done with different trains (8 bunches, 16 bunches, 24 bunches) show that the charge is always below 2nC/bunch. A proposal [4] was made in order to produce high charges at the RF gun with long laser pulses (σ_t = 8 ps). They will be accelerated up to 10 MeV/c (or even 20 MeV/c later on) and then longitudinally compressed down to σ_t = 3 ps.

This note describes the principle of the magnetic bunch compressor based on 3 dipoles. The optics and the settings of the whole CTF line are given. Finally the beam dynamics simulations are analysed and show that the bunch characteristics at the compressor output can be conserved up to the CLIC structure with a good efficiency.

2 Analytical model

2.1 Variable definitions

A group of particles are described by two sets of canonically conjugate variables $\dot{q}$ and $\dot{p}$. If the system is conservative, one can derive the classical particle motion from the Hamiltonian function $H(q,p,t)$

$$\dot{q} = \frac{\partial H}{\partial p} \tag{1}$$

$$\dot{p} = -\frac{\partial H}{\partial q} \tag{2}$$

Under these conditions the particles move in the phase space as in an incompressible fluid. The Hamiltonian function for a charged particle of mass, m, and charge, e, in a magnetic vector potential $\vec{A}$, and scalar potential, ϕ, is:

$$H = c\Phi + c\sqrt{(\vec{p} - e\vec{A})^2 + m^2c^2} \tag{3}$$

where

Φ and $\vec{A}$ are function of space and time,
c is the velocity of the light,
$\vec{q} = q_x, q_y, q_z$ is the space coordinate,
$\vec{p} = p_x, p_y, p_z$ is the momentum conjugate to the space coordinate.

From (1) and (2) and expanding the equation (3) one obtains:

$$\dot{q}_i = \frac{c(p_i - eA_i)}{\sqrt{(\vec{p} - e\vec{A})^2 + m^2c^2}} \tag{4}$$

and

$$\dot{p}_i = -e\frac{\partial \Phi}{\partial q_i} + ec\sum_j \frac{p_j - eA_j}{\sqrt{(\vec{p} - e\vec{A})^2 + m^2c^2}}\frac{\partial A_j}{\partial q_i} \tag{5}$$

which gives

$$\dot{p}_i - e\dot{A}_i = -e\frac{\partial \Phi}{\partial q_i} - e\frac{\partial A_i}{\partial t} + e\sum_j (\dot{q}_j \frac{\partial A_j}{\partial \dot{q}_i} - qj\frac{\partial A_i}{\partial q_j}) \tag{6}$$

From equation (4), the normalized velocity $\dot{q}/c$ can be written as:

$$\beta^2 = \frac{(\vec{p} - e\vec{A})^2}{(\vec{p} - e\vec{A})^2 + m^2c^2} \tag{7}$$

that one develops to get:

$$p_i - eA_i = \beta_i \gamma mc \tag{8}$$

Only the longitudinal plane will be discussed here. Additionally, the equation (8) will be considered where $A_x = A_z = 0$ [5]. Under this hypothesis (8) becomes:

$$p_z = \beta_z \gamma mc \tag{9}$$

where $\beta_z = \dot{q}_z/c$

This transformation shows that the behaviour of the longitudinal plane is the same as the transverse plane in a sense that if the system is conservative then there exists a phase space described by a set of two conjugate variables $(q_z, \beta_z\gamma)$ in which the longitudinal emittance is conserved (Liouville's theorem).

2.2 Equivalence between particle phase Φ and longitudinal position z

The bunch compression studies are simulated with the code PARMELA [6] in which the accessible longitudinal variables are $(\Phi, \beta_z\gamma)$. The linear relation between ϕ and z [1] is recalled below. The phase of the particle i is usually defined as $\Phi_i = -\omega(t_i - t_0) + \Phi_0$ as the phase of a particle i relativistic or not [7], where

$t_i = z_i/v_i$,
$\omega = 2\pi c/\lambda$,
λ is the wavelength associated to the RF,
v_i is the velocity of the particle,
t_0 is the time of the reference particle,
Φ_0 is the phase of the reference particle.

[1] For simplicity the variable q_z from the Hamiltonian formalism is renamed z.

This yields to:

$$\Phi_i = -\frac{2\pi}{\lambda} c\left(\frac{z_i}{v_i} - \frac{z_0}{v_0}\right) + \Phi_0 \tag{10}$$

If z_0 is the longitudinal position of the reference particle in the bunch, then the longitudinal position of the particle i becomes $z_i = z_0 + \Delta z$. The expansion of (10) provides:

$$\Phi_i = -\frac{2\pi}{\lambda}\left(\frac{\Delta z}{\beta_i} - z_0\left(\frac{1}{\beta_0} - \frac{1}{\beta_i}\right)\right) + \Phi_0 \tag{11}$$

The bunch compressor will work, at least, at 11 MeV, then particles will be relativistic: $\beta_i = \beta_0 \simeq 1$ and

$$\Delta\Phi = -\frac{2\pi\Delta z}{\lambda} \tag{12}$$

Finally, the variables $(\Phi, \beta_z\gamma)$ are also a set of conjugate variables and the particle behaviour is the same as in $(z, \beta_z\gamma)$.

2.3 Principle of the longitudinal compression

The previous paragraphs demonstrated that the longitudinal emittance is conserved either in the $(z, \beta_z\gamma)$ or $(\Phi, \beta_z\gamma)$ phase spaces. A general formalism of the longitudinal compression is given below.

First, let us consider an ellipse in one of those phase spaces containing ninety per cent of particles for example, where their coordinates and momentum are taken as a function of the reference particle: $z_0 = 0$, $t_0 = 0$ and $(\beta_z\gamma)_0$.

In all the following figures the phase spaces are centred in phase and momentum on the reference particle.

Therefore $\Delta z = z_i - z_0 = z_i$, $\Delta\phi = \phi_i - \phi_0 = \phi_i$ and $\delta p \simeq ((\beta_z\gamma)_i - (\beta_z\gamma)_0 \longrightarrow (\beta_z\gamma)_i$. The area ϵ of the ellipse, which also represents the beam emittance, is described by a linear combination of a generalisation of the Twiss parameters $(\alpha_l, \beta_l, \gamma_l)$ as it is done for the transverse plane:

$$\gamma_l {z_i}^2 + 2\alpha_l z_i (\beta_z\gamma)_i + \beta_l (\beta_z\gamma)_i^2 = \epsilon_z \tag{13}$$

Let $\eta = -2\pi/\lambda$ in (12). Then (13) can be written as:

$$\gamma_l \frac{{\Phi_i}^2}{\eta^2} + 2\frac{\alpha_l \Phi_i}{\eta}(\beta_z\gamma)_i + \beta_l (\beta_z\gamma)_i^2 = \epsilon_\Phi \tag{14}$$

One can compare both emittances by comparing the surfaces of the straight ellipses (coupling term α_l=0).

$$S_z = \pi\beta_l\gamma_l$$

$$S_\Phi = \pi\frac{\beta_l\gamma_l}{\eta^2}$$

and

$$S_\Phi = \frac{S_z}{\eta^2}$$

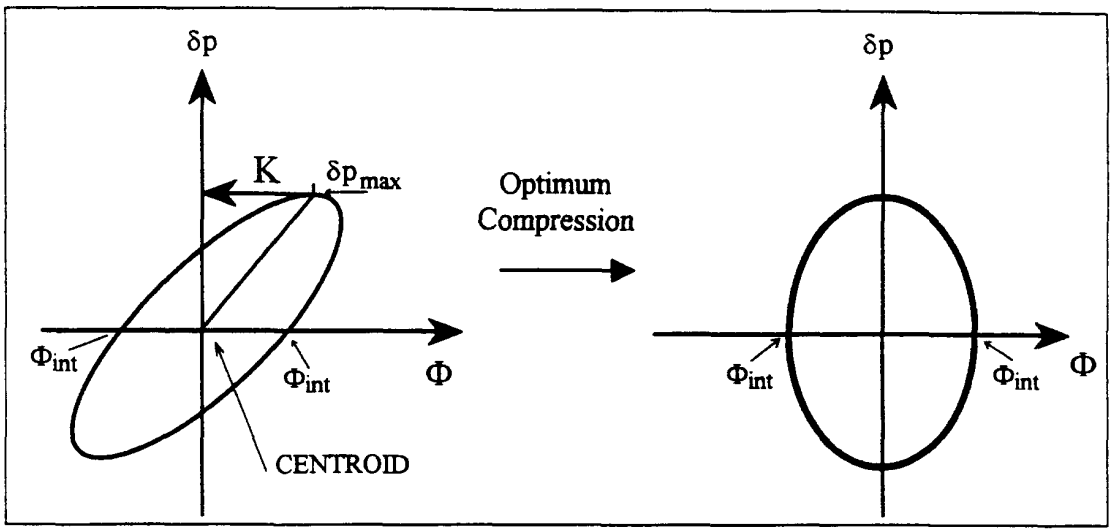

Figure 1: Compression process in the $(\Phi, \delta p)$ phase space

The emittance being proportional to the surfaces, one obtains:

$$\epsilon_\Phi = \frac{\epsilon_z}{\eta^2} \tag{15}$$

From now on, the phase space $(\phi, \beta_z\gamma)$ will be used. Let us apply to the ellipse the following adiabatic transformation (Fig. 1):

$$\begin{cases} \Phi_s = \Phi_e - K(\beta_z\gamma)_e \\ (\beta_z\gamma)_s = (\beta_z\gamma)_e \end{cases} \tag{16}$$

where the index, e, refers to the quantities before the transformation and the index, s, refers to the quantities after the transformation. K is an arbitrary constant (positive or negative). This transformation conserves the momentum of the particle but modifies its phase. It is also a linear transformation which implies a correlation between Φ and $\beta_z\gamma$. For a given correlation, K should be determined in a such way that the change in phase is proportional to the momentum. Therefore the phase spread in the bunch will tend to a minimum.

The equation (14) of the ellipse after the compression process becomes:

$$\gamma_l\frac{\Phi_s}{\eta^2} + 2(\frac{\alpha_l}{\eta} + \frac{\gamma_l K}{\eta^2})\Phi_s(\beta_z\gamma) + (\frac{\gamma_l K}{\eta^2} + 2\frac{\alpha_l K}{\eta} + \beta_l)(\beta_z\gamma)^2 = \epsilon_\Phi \tag{17}$$

For a more readable equation let put $\gamma_l/\eta^2 \rightarrow \gamma_l$, $\alpha_l/\eta \rightarrow \alpha_l$ and $\epsilon_\Phi \rightarrow \epsilon$, so the equation (17) becomes:

$$\gamma_l\Phi_s + 2(\alpha_l + \gamma_l K)\Phi_s(\beta_z\gamma) + (\gamma_l K + 2\alpha_l K + \beta_l)(\beta_z\gamma)^2 = \epsilon \tag{18}$$

The optimum compression is reached when the ellipse has a horizontal waist. This condition gives immediately a unique value of K:

$$K = -\frac{\alpha_l}{\gamma_l} \tag{19}$$

2.4 Minimum bunch length

The ellipse parameters (Fig. 2) for the longitudinal phase plane are derived from [8]. The relation between K and these parameters is given below.

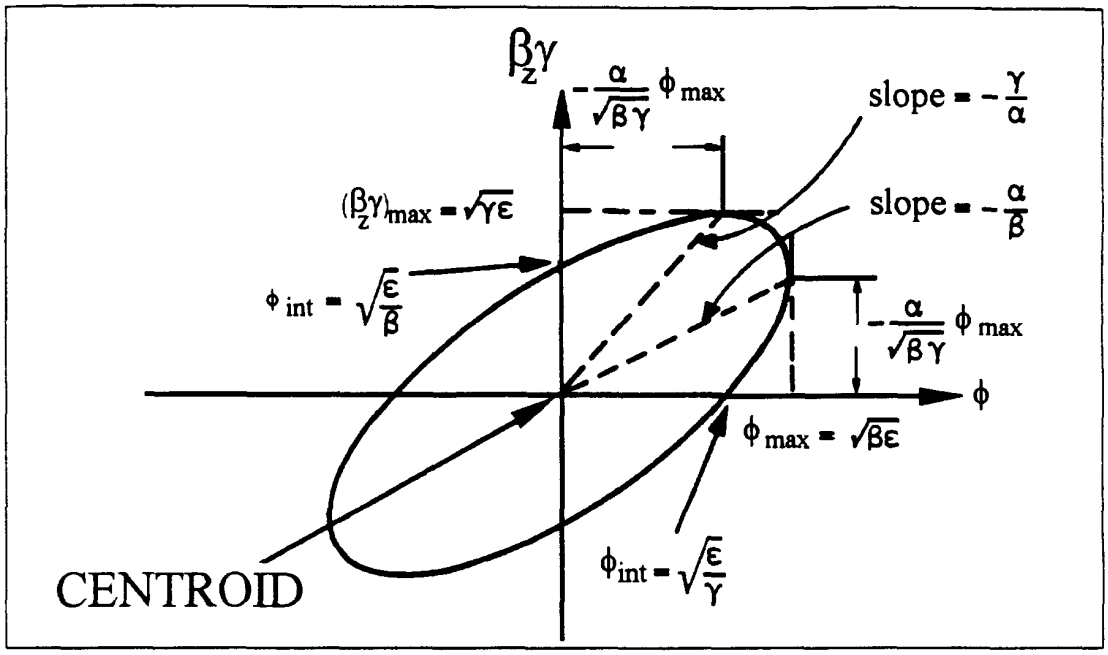

Figure 2: Ellipse parameters for the longitudinal phase plane.

Assuming that K depends on the position of $(\beta_z\gamma)_{max}$, the transformation (16) yields:

$$\Phi_s = \Phi_e - K(\beta_z\gamma)_{max} = 0 \tag{20}$$

The phase associated to $(\beta_z\gamma)_{max}$ is Φ_e which can be developed into:

$$\Phi_e = -\frac{\alpha_l}{\sqrt{\beta_l\gamma}}\Phi_{max} \Longrightarrow \Phi_e = -\alpha_l\sqrt{\frac{\epsilon}{\gamma_l}}$$

and

$$(\beta_z\gamma)_{max} = \sqrt{\gamma_l\epsilon}$$

By substituting the expression of Φ_e into (20), one obtains:

$$-\alpha_l\sqrt{\frac{\epsilon}{\gamma_l}} - K\sqrt{\gamma_l\epsilon} = 0 \Longrightarrow K = -\frac{\alpha_l}{\gamma_l} \tag{21}$$

Therefore, $(\beta_z\gamma)_{max}$ is the ellipse reference point for an optimum compression and every time this point will change, so will K. Similarly, two points will determine, theoretically, the minimum phase spread of the bunch: ϕ_{int} and its symmetric from the vertical axis. Then the minimum bunch length is:

$$\Delta\phi = 2\phi_{int} = 2\sqrt{\frac{\epsilon}{\gamma_l}} \tag{22}$$

Because of the Liouville's theorem the positions of ϕ_{int} can still be reduced by increasing the momentum spread ($\sim \gamma_l$ increases) for a constant emittance. Then, ideally, ϕ_{int} would be reduced to zero if $\delta p/p \rightarrow \infty$.

2.5 Magnetic compression with three dipoles

For the reasons explained in Section 2.9.5, the choice for the CTF line is settled for a system of three dipoles of inverse polarity. A study of such system is given below.

2.5.1 Optical design

This layout allows to keep the same momentum spread before and after the compression process. The following analytical study will not integrate the effect of the dipole fringe fields, only hard edge field is assumed. In the general case, a beam enters into the bunch compressor system with an angle ϵ (Fig. 3). Its trajectory through those dipoles depends of eleven quantities:

$l_{i=1..3}$: the length of each dipole,
α, β, γ: the curvature angle of each dipole,
$\rho_{i=1..3}$: the curvature radius of the dipole,
$\lambda_{i=1,2}$: the drift between the dipoles.

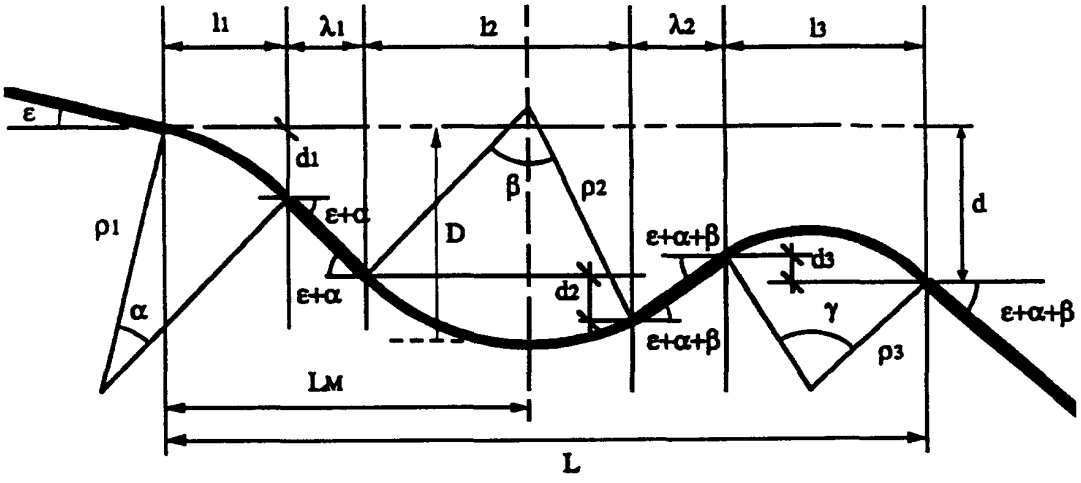

Figure 3: Basic geometry for a 3 dipole bunch compressor.

■ Magnet lengths (Fig. 4 and 5).

$$l_1 = \rho_1[\sin(\epsilon + \alpha) - \sin\epsilon] \tag{23}$$

$$l_2 = \rho_2[\sin(\epsilon + \alpha) - \sin(\epsilon + \alpha + \beta)] \tag{24}$$

$$l_3 = \rho_3[\sin(\epsilon + \alpha + \beta + \gamma) - \sin(\epsilon + \alpha + \beta)] \tag{25}$$

The total length of the bunch compressor is:

$$L = l_1 + l_2 + l_3 + \lambda_1 + \lambda_2 \tag{26}$$

■ In the transverse plane: d_i = offset in position between the input and the output of the dipoles.

$$d_1 = \rho_1[\cos\epsilon - \cos(\epsilon + \alpha) \tag{27}$$

$$d_2 = \rho_2[\cos(\epsilon + \alpha + \beta) - \cos(\epsilon + \alpha)] \tag{28}$$

$$d_3 = \rho_3[\cos(\epsilon + \alpha + \beta) - \cos(\epsilon + \alpha + \beta + \gamma)] \tag{29}$$

The total offset in position between the input and the output of the bunch compressor in the transverse plane is:

$$d = d_1 + d_2 + d_3 + \lambda_1 \tan(\epsilon + \alpha) + \lambda_2 \tan(\epsilon + \alpha + \beta)]$$

The problem is simplified as follow:

$$\epsilon = 0 \text{ and } \epsilon + \alpha + \beta + \gamma = 0$$

assuming the beam to be parallel to the z-axis at the entrance and the exit of the bunch compressor system. Then

$$\beta = -(\alpha + \gamma) \Longrightarrow \gamma = \alpha \Longrightarrow \boxed{\beta = -2\alpha} \tag{30}$$

Additionally, we settle d to zero for reasons of symmetry:

$$d = (\rho_1 + \rho_2)(1 - \cos\alpha) + (\lambda_1 + \lambda_2)\tan\alpha = 0 \tag{31}$$

Still willing to keep a symmetrical system we take:

$$\boxed{\rho_1 = \rho_2 = \rho_3 = \rho \text{ and } \lambda_1 = \lambda_2 = \lambda} \tag{32}$$

■ Maximum transverse displacement:

$$\boxed{D = 2\rho(1 - \cos\alpha) + \lambda\tan\alpha} \tag{33}$$

■ Longitudinal position associated to the maximum transverse deflection:

$$\boxed{L_M = 2\rho\sin\alpha + \lambda} \tag{34}$$

With the mentioned simplifications, the expressions of the lengths become:

$$l_1 = \rho\sin\alpha \tag{35}$$

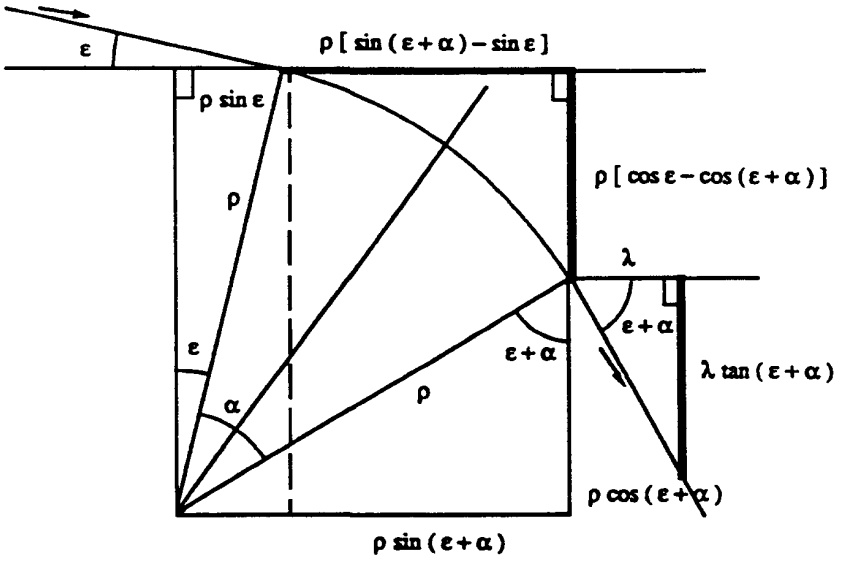

Figure 4: First dipole parameters.

(The third dipole is the same.)

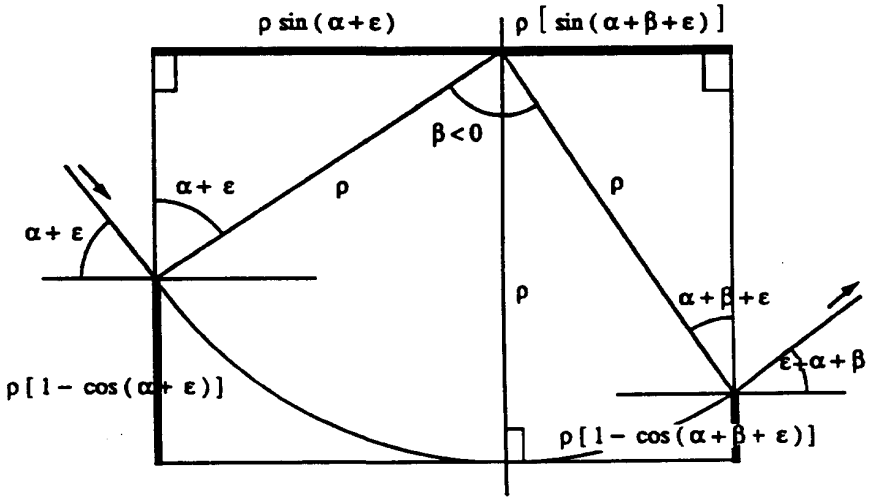

Figure 5: Second dipole parameters

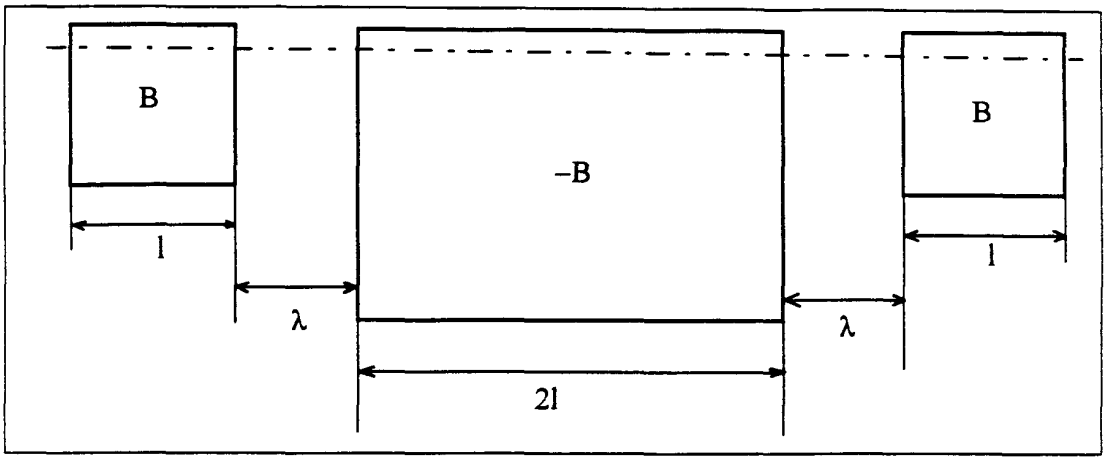

Figure 6: Basic requirements for a simplified bunch compressor.

$$l_2 = \rho[\sin\alpha - \sin(-\alpha)] = 2\rho\sin\alpha \tag{36}$$

$$l_3 = \rho[\sin(\alpha+\beta+\gamma) - \sin(\alpha+\beta)] = \rho\sin\alpha \tag{37}$$

Therefore:

$$\boxed{2l_1 = 2l_3 = l_2 = 2l} \tag{38}$$

Since $\rho = l/\sin\alpha$ and $B_{[T]}\rho_{[m]} \approx P_{[GeV/c]}/0.299$, there is the following relations between the fields:

$$\boxed{B_1 = B_2 = B_3 = B} \tag{39}$$

Figure 6 gives the simplified scheme.

2.5.2 Horizontal matrix for beam optics

The symmetry conditions for the lengths and magnetic field (Fig. 6) are used to develop the matrix formalism. The bunch compressor is composed of three elementary matrices: a dipole $[B]$, an edge focusing $[F]$ and a drift $[D]$. Each of them will describe the motion in a 4x4 matrix formalism for the horizontal plane [8].

$$\begin{bmatrix} x \\ x' \\ \delta l_p \\ \delta p/p \end{bmatrix}_1 = \left[MATRIX\right] \begin{bmatrix} x \\ x' \\ \delta l_p \\ \delta p/p \end{bmatrix}_0$$

The [MATRIX] elements are:

$$[B] = \begin{bmatrix} \cos\alpha & \rho\sin\alpha & 0 & \rho(1-\cos\alpha) \\ -\sin\alpha/\rho & \cos\alpha & 0 & \sin\alpha \\ -\sin\alpha & -\rho(1-\cos\alpha) & 1 & -\rho(\alpha-\sin\alpha) \\ 0 & 0 & 0 & 1 \end{bmatrix}$$

$$[F] = \begin{bmatrix} 1 & 0 & 0 & 0 \\ \tan\alpha/\rho & 1 & 0 & 0 \\ 0 & 0 & 1 & 0 \\ 0 & 0 & 0 & 1 \end{bmatrix}$$

$$[D] = \begin{bmatrix} 1 & \lambda & 0 & 0 \\ 0 & 1 & 0 & 0 \\ 0 & 0 & 1 & 0 \\ 0 & 0 & 0 & 1 \end{bmatrix}$$

The variables are:

x, x' : horizontal position and divergence,
δl_p : path length difference between the arbitrary ray and the central trajectory,
$\delta p/p$: relative momentum spread.

We will use the following notations to lighten the matrix expressions:

C as $\cos\alpha$
S as $\sin\alpha$
T as $\tan\alpha$

The edge focusing has no effect on a beam perpendicular to the dipole edge, then the matrix calculation will begin and end with one dipole matrix.

The central magnet $[FBBF]$ will be composed of two identical magnets of curvature angle, $-\alpha$, and curvature radius, ρ, giving a total curvature angle of -2α. Because of their reversed sign, the matrix of the central magnet will be taken as if it were positive and reversed after calculation.

Calculation of [DFB] for the first dipole:

$$[FB] = \begin{bmatrix} 1 & 0 & 0 & 0 \\ T/\rho & 1 & 0 & 0 \\ 0 & 0 & 1 & 0 \\ 0 & 0 & 0 & 1 \end{bmatrix} \begin{bmatrix} C & \rho S & 0 & \rho(1-C) \\ -S/\rho & C & 0 & S \\ -S & -\rho(1-C) & 1 & -\rho(\alpha-S) \\ 0 & 0 & 0 & 1 \end{bmatrix}$$

$$[FB] = \begin{bmatrix} C & \rho S & 0 & \rho(1-C) \\ 0 & TS+C & 0 & T(1-C)+S \\ -S & -\rho(1-C) & 1 & -\rho(\alpha-S) \\ 0 & 0 & 0 & 1 \end{bmatrix} = \begin{bmatrix} C & \rho S & 0 & \rho(1-C) \\ 0 & 1/C & 0 & T \\ -S & -\rho(1-C) & 1 & -\rho(\alpha-S) \\ 0 & 0 & 0 & 1 \end{bmatrix}$$

$$[DFB] = \begin{bmatrix} 1 & \lambda & 0 & 0 \\ 0 & 1 & 0 & 0 \\ 0 & 0 & 1 & 0 \\ 0 & 0 & 0 & 1 \end{bmatrix} [FB] = \begin{bmatrix} C & \rho S + \lambda/C & 0 & \rho(1-C)+\lambda T \\ 0 & 1/C & 0 & T \\ -S & -\rho(1-C) & 1 & -\rho(\alpha-S) \\ 0 & 0 & 0 & 1 \end{bmatrix} \quad (40)$$

Calculation of [FBBF] for the second dipole:

$$[FBBF] = \begin{bmatrix} C & \rho S & 0 & \rho(1-C) \\ 0 & 1/C & 0 & T \\ -S & -\rho(1-C) & 1 & -\rho(\alpha - S) \\ 0 & 0 & 0 & 1 \end{bmatrix} \begin{bmatrix} C & \rho S & 0 & \rho(1-C) \\ -S/\rho & C & 0 & S \\ -S & -\rho(1-C) & 1 & -\rho(\alpha - S) \\ 0 & 0 & 0 & 1 \end{bmatrix} \begin{bmatrix} 1 & 0 & 0 & 0 \\ T/\rho & 1 & 0 & 0 \\ 0 & 0 & 1 & 0 \\ 0 & 0 & 0 & 1 \end{bmatrix}$$

$$[FBBF] = \begin{bmatrix} \cdots \end{bmatrix} \begin{bmatrix} C + S^2/C & \rho S & 0 & \rho(1-C) \\ -S/\rho + S/\rho & C & 0 & S \\ -S - T(1-C) & -\rho(1-C) & 1 & -\rho(\alpha - S) \\ 0 & 0 & 0 & 1 \end{bmatrix}$$

$$[FBBF] = \begin{bmatrix} \cdots \end{bmatrix} \begin{bmatrix} 1/C & \rho S & 0 & \rho(1-C) \\ 0 & C & 0 & S \\ -T & -\rho(1-C) & 1 & -\rho(\alpha - S) \\ 0 & 0 & 0 & 1 \end{bmatrix}$$

$$[FBBF] = \begin{bmatrix} 1 & 2\rho CS & 0 & \rho C(1-C) + \rho S^2 + \rho(1-C) \\ 0 & 1 & 0 & 2T \\ -2T & -\rho S^2 - \rho C(1-C) - \rho(1-C) & 1 & -2\rho S(1-C) - 2\rho(\alpha - S) \\ 0 & 0 & 0 & 1 \end{bmatrix}$$

Finally,

$$[FBBF] = \begin{bmatrix} 1 & 2\rho CS & 0 & 2\rho S^2 \\ 0 & 1 & 0 & 2T \\ -2T & -2\rho S^2 & 1 & -2\rho(\alpha - SC) \\ 0 & 0 & 0 & 1 \end{bmatrix} \tag{41}$$

We apply now the transformation due to the reversed angle and reverse curvature radius:

$$[FBBF]_{trans} = \begin{bmatrix} 1 & 2\rho CS & 0 & -2\rho S^2 \\ 0 & 1 & 0 & -2T \\ 2T & 2\rho S^2 & 1 & 2\rho(-\alpha + SC) \\ 0 & 0 & 0 & 1 \end{bmatrix} \tag{42}$$

Calculation of [BFD] for the third dipole:

$$[BFD] = \begin{bmatrix} 1/C & \rho S & 0 & \rho(1-C) \\ 0 & C & 0 & S \\ -T & -\rho(1-C) & 1 & -\rho(\alpha - S) \\ 0 & 0 & 0 & 1 \end{bmatrix} \begin{bmatrix} 1 & \lambda & 0 & 0 \\ 0 & 1 & 0 & 0 \\ 0 & 0 & 1 & 0 \\ 0 & 0 & 0 & 1 \end{bmatrix} \tag{43}$$

$$[BFD] = \begin{bmatrix} 1/C & \rho S + \lambda/C & 0 & \rho(1-C) \\ 0 & C & 0 & S \\ -T & -\rho(1-C) - \lambda T & 1 & -\rho(\alpha - S) \\ 0 & 0 & 0 & 1 \end{bmatrix} \tag{44}$$

Calculation of the whole matrix transformation:

$$[BFD][FBBF]_{trans}[DFB] =$$

$$[BFD]\begin{bmatrix} C & \rho S+\frac{\lambda}{C}+2\rho S & 0 & \rho(1-C)+\lambda T+2\rho S^2-2\rho S^2 \\ 0 & 1/C & 0 & T-2T \\ 2S-S & 2T(\rho S+\frac{\lambda}{C}) & 1 & 2T(\rho(1-C)+\lambda T)+2\rho TS^2-\rho(\alpha-S)-2\rho(\alpha-SC) \\ 0 & 0 & 0 & 1 \end{bmatrix}$$

Which becomes,

$$=[BFD]\begin{bmatrix} C & 3\rho S+\frac{\lambda}{C} & 0 & \rho(1-C)+\lambda T \\ 0 & 1/C & 0 & -T \\ S & 4T\rho S+\frac{2T\lambda}{C}-\rho(1-C) & 1 & 2T(\rho(1-C)+\lambda T)+2\rho TS^2-\rho(\alpha-S)-2\rho(\alpha-SC) \\ 0 & 0 & 0 & 1 \end{bmatrix}$$

Let: $A=2T(\rho(1-C)+\lambda T)+2\rho TS^2-\rho(\alpha-S)-2\rho$
and $B=\frac{\rho}{C}(1-C)+\frac{\lambda T}{C}-\frac{\lambda T}{C}-\rho TS+\rho(1-C)$

$$=\begin{bmatrix} 1 & 3\rho T+\frac{2\lambda}{C^2}+\rho T & 0 & B \\ 0 & 1 & 0 & -CT+S \\ 0 & -3T\rho S-\frac{\lambda T}{C}-\frac{\lambda T}{C}-\frac{\rho}{C}(1-C)+4\rho TS+\frac{2T\lambda}{C}-\rho(1-C) & 1 & A-\rho(\alpha-S) \\ 0 & 0 & 0 & 1 \end{bmatrix}$$

$$[BFD][FBBF]_{trans}[DFB]=\begin{bmatrix} 1 & 4\rho T+\frac{2\lambda}{C^2} & 0 & 0 \\ 0 & 1 & 0 & 0 \\ 0 & 0 & 1 & 4\rho(T-\alpha)+2\lambda T^2 \\ 0 & 0 & 0 & 1 \end{bmatrix} \tag{45}$$

Since δl_0 and δl_1 are respectively the initial and final distance between an arbitrary particle and the central particle, Δl_p is the relative lengthening or shortening of the distance between both particles.

This formalism can be extended to a bunch of particles in which one has to characterise the central particle and the arbitrary particle. We can now express these quantities function of the momentum spread:

$$\delta l_1-\delta l_0=\Delta l_p=[4\rho(\tan\alpha-\alpha)+2\lambda\tan^2\alpha]\frac{\delta p}{p} \qquad [\text{mm}] \tag{46}$$

with $\rho=l/\sin\alpha$. Δl_p could be expressed in degrees. Since 100 mm correspond to 360 degrees for our RF, then:

$$\frac{\Delta\phi}{\frac{\delta p}{p}}=\frac{360}{100}\frac{\Delta l_p}{\frac{\delta p}{p}} \qquad [\text{degree}/\%] \tag{47}$$

Table 1 gives numerical values of these quantities for l=150 mm and λ=100 mm:

α [degree]	$\frac{\Delta l_p}{\frac{\Delta p}{p}}$[mm/%]	$\frac{\Delta\phi}{\frac{\Delta p}{p}}$ [degree/%]	B[T] at 11MeV/c	B[T] at 20 MeV/c
5	0.03	0.11	0.021	0.039
10	0.12	0.45	0.043	0.077
15	0.29	1.03	0.064	0.115
20	0.53	1.89	0.084	0.152
25	0.86	3.09	0.104	0.188
30	1.31	4.72	0.123	0.223
35	1.92	6.89	0.141	0.256
40	2.72	9.80	0.158	0.287
45	3.82	13.76	0.173	0.315
50	5.34	19.22	0.188	0.342
55	7.51	27.03	0.201	0.365
60	10.74	38.68	0.212	0.386
65	15.88	57.18	0.222	0.404

Table 1: α-dependence of main parameters

2.5.3 Vertical matrix for beam optics

The same matrix transformation $[BFD][FBBF]_{trans}[DFB]$ for the vertical plane is computed.
y, y': vertical position and divergence.

$$[BF] = \begin{bmatrix} 1 & \rho\alpha \\ 0 & 1 \end{bmatrix} \begin{bmatrix} 1 & 0 \\ -T/\rho & 1 \end{bmatrix} = \begin{bmatrix} 1-\alpha T & \rho\alpha \\ -T/\rho & 1 \end{bmatrix}$$

$$[FB] = \begin{bmatrix} 1 & 0 \\ -T/\rho & 1 \end{bmatrix} \begin{bmatrix} 1 & \rho\alpha \\ 0 & 1 \end{bmatrix} = \begin{bmatrix} 1 & \rho\alpha \\ -T/\rho & 1-\alpha T \end{bmatrix}$$

$$[BFD] = \begin{bmatrix} 1-\alpha T & \rho\alpha \\ -T/\rho & 1 \end{bmatrix} \begin{bmatrix} 1 & \lambda \\ 0 & 1 \end{bmatrix} = \begin{bmatrix} 1-\alpha T & \lambda(1-\alpha T)+\rho\alpha \\ -T/\rho & 1-\lambda T/\rho \end{bmatrix}$$

$$[DFB] = \begin{bmatrix} 1 & \lambda \\ 0 & 1 \end{bmatrix} \begin{bmatrix} 1-\alpha T & \rho\alpha \\ -T/\rho & 1 \end{bmatrix} = \begin{bmatrix} 1-\lambda T/\rho & \lambda(1-\alpha T)+\rho\alpha \\ -T/\rho & 1-\alpha T \end{bmatrix}$$

$$[FBBF] = \begin{bmatrix} 1 & \rho\alpha \\ -T/\rho & 1-\alpha T \end{bmatrix} \begin{bmatrix} 1-\alpha T & \rho\alpha \\ -T/\rho & 1 \end{bmatrix} = \begin{bmatrix} 1-2\alpha T & 2\rho\alpha \\ -2T(1-\alpha T)/\rho & 1-2\alpha T \end{bmatrix}$$

Finally, the matrix transformation for the vertical plane is:

$$[BFD][FBBF]_{trans}[DFB] = \left[\begin{array}{cc} 1+8(\alpha T)^2-8\alpha T & 4\rho\alpha(1-\alpha T)(1-2\alpha T) \\ +2\lambda^2(T/\rho)^2(1\alpha T)^2 & -2\lambda^2 T/\rho(1-\alpha T)^3 \\ -4\lambda(T/\rho)(1-\alpha T)(1-2\alpha T) & +2\lambda(1-\alpha T)^2(1-4\alpha T) \\ \hline 4(T/\rho)(2\alpha T-1) & 1+8(\alpha T)^2-8\alpha T \\ -2\lambda^2(T/\rho)^3(1-\alpha T) & +2\lambda^2(T/\rho^2(1-\alpha T)^2 \\ +2\lambda(T/\rho)^2(3-4\alpha T) & -4\lambda(T/\rho(1-\alpha T)(1-2\alpha T) \end{array}\right]$$

In the vertical plane, the focusing effect is given by:

$$f = \frac{1}{4(T/\rho)(2\alpha T-1) - 2\lambda^2(T/\rho)^3(1-\alpha T) + 2\lambda(T/\rho)^2(3-4\alpha T)} \tag{48}$$

2.6 Spectrometer optics

With the bunch compressor design, a spectrometer line will be implemented. The first dipole is switched on while the two others are off. From (40), the horizontal beam size at the exit of the first dipole is:

$$x_1 = x_0\cos\alpha + x'_0(\rho\sin\alpha + \frac{\lambda}{\cos\alpha}) + [\rho(1-\cos\alpha) + \lambda\tan\alpha]\frac{\delta p}{p} \tag{49}$$

The first two terms are the emittance contribution ($Sigma_x$).
The third term is the dispersion contribution ($Disp$).
From both quantities, the resolution of the spectrometer is derived:

$$f(\lambda) = \frac{[\rho(1-\cos\alpha) + \lambda\tan\alpha]\frac{\delta p}{p}}{x_0\cos\alpha + x_0'(\rho\sin\alpha + \frac{\lambda}{\cos\alpha})} \tag{50}$$

Figure 7 shows the evolution of $f(\lambda)$ for a beam with the following characteristics taken from the output data of PARMELA at the exit of the first dipole magnet at 0 nC:

Momentum spread: $\frac{\delta p}{p}$=3.8%,
one-half of the horizontal beam extent: x_0=1.3 mm,
one-half of the horizontal beam divergence: x'_0=2.4 mrad,
the curvature angle of the spectrometer: α=30 degrees.

From this figure a possible position of the screen around 1 m is possible since the resolution curve $f(\lambda)$ starts to saturate.

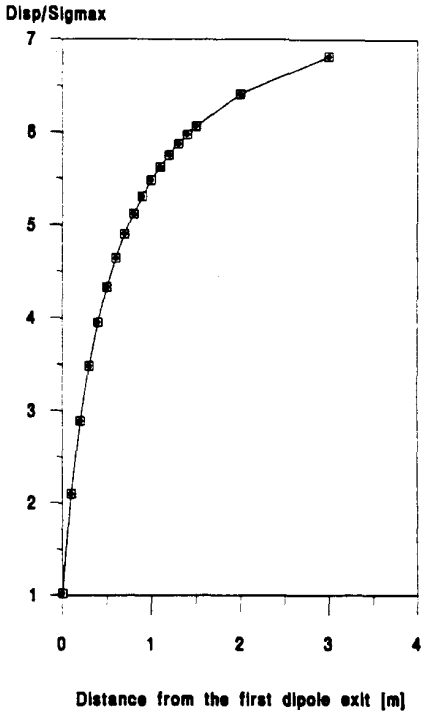

Figure 7: Spectrometer resolution

2.7 Ellipse parameters in the longitudinal phase space

From (46) and (47):

$$\phi_1 - \phi_0 = \frac{360}{100}[4\rho(\tan\alpha - \alpha) + 2\lambda\tan^2\alpha]\frac{\delta p}{p} \qquad [\text{deg.}\%] \tag{51}$$

As written previously for the path length (see 2.5), ϕ_1-ϕ_0 represents the relative lengthening or shortening of the phase extension of the bunch. Once the momentum spread known one can vary the relative phase extension by changing the parameters of the bunch compressor: α, ρ, λ.

An optimum compression is obtained for ϕ_1=0, the two particles have the same phase. Then, one has to know the initial value ϕ_0 to calculate (51). (20) gives this information. One can note that both quantities ϕ_0 and ϕ_e are the same and with (20), one has:

$$K = \frac{\phi_e}{(\beta_z\gamma)_{max}} \tag{52}$$

We have now to establish a relation between (52) and (51) at $(\delta p/p)_{max}$ to determine the expression of α and the magnetic field. For this purpose and since $(\beta_z\gamma)_{max}$ is the point

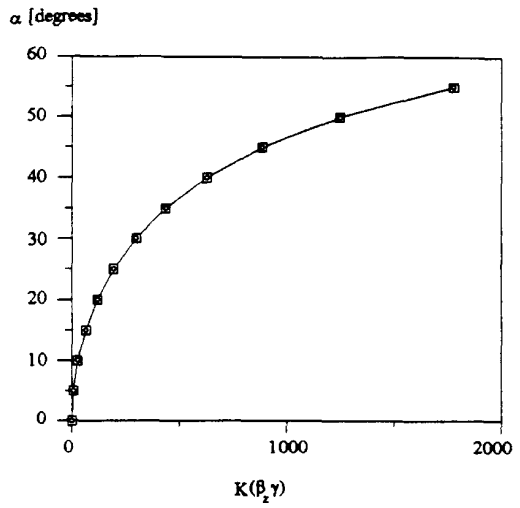

Figure 8: Evolution of α function of $K(\beta_z\gamma)_0$

for an optimum compression (Fig. 1), we express the momentum spread function of this particular point of the ellipse:

$$(\delta p/p)_{max} = (p_{max} - p_0)/p_0 = ((\beta_z\gamma)_{max} - (\beta_z\gamma)_0)/(\beta_z\gamma)_0 = \delta(\beta_z\gamma)_{max}/(\beta_z\gamma)_0$$

Using the equations (35) and (52), and since the ellipse is centred around the reference particle $\delta(\beta_z\gamma)_{max} \longrightarrow (\beta_z\gamma)_{max}$, the equation (51) becomes:

$$\frac{\phi_1 - \phi_0}{(\beta_z\gamma)_{max}/(\beta_z\gamma)_0} = [4l(\frac{\tan\alpha - \alpha}{\sin\alpha}) + 2\lambda\tan^2\alpha]\frac{360}{100} = K(\beta_z\gamma)_0 \qquad (53)$$

To resolve this equation where α is unknown, a numerical method is used. Finally, another computation will be required to extract the α value from (53). Figure 8 shows α versus $K(\beta_z\gamma)_0$. Each different value of K is determined by the initial conditions of the bunch. For example, at 0 nC, $K(\beta_z\gamma)_0 = 298.0$ then a curvature angle of $\alpha = 30$ degrees would have to be applied to this bunch, corresponding to a magnetic field of $B = 0.222$ Tesla for a 20 MeV beam.

2.8 RMS beam emittance

PARMELA code gives an arbitrary longitudinal particle distribution before the bunch compressor system. An ellipse fitting the rms values of the distribution can be deduced. The description of this ellipse is the same as in paragraph 2.3. The rms emittance ϵ_{RMS} [9] is described as follow:

$$< (\beta_z\gamma)^2 >= \gamma_l\epsilon_{RMS}$$

$$< \phi(\beta_z\gamma) >= -\alpha_l\epsilon_{RMS}$$

$$< \phi^2 >= \beta_l\epsilon_{RMS}$$

$$\epsilon_{RMS} = \sqrt{< \phi^2 >< (\beta_z\gamma)^2 > - < \phi(\beta_z\gamma) >^2}$$

where angle brackets indicate averages of the bracketed quantities over the entire bunch. One can express them with the help of the variable x for simplicity. The *mean* of the values $x_1, \cdots, x_N$ is:

$$< x >= \frac{1}{N}\sum_{j=1}^{N} x_j$$

and the *variance*:

$$Var(x_1 \cdots x_N) =< x^2 >= \frac{1}{N-1}\sum_{j=1}^{N}(x_j - < x >)^2$$

or its square root, the standard deviation:

$$\sigma(x_1 \cdots x_N) = \sqrt{Var(x_1 \cdots x_N)}$$

2.9 Review of other magnetic compressions

There exists numerous ways and systems to compress an electron bunch [10], [11] and [12]. Three of them are mentioned here as possible bunch compressors for CTF: planar wiggler, helical wiggler, alpha-magnet. The two wigglers are similar to the magnetic chicane and will be quantitatively compare to it.

2.9.1 Chicane

Under the paraxial condition [13], $\beta_\parallel \simeq c$, the difference of path length is given by:

$$\Delta l_c \propto \frac{l^3}{p^2}(eB_0)^2\frac{\delta p}{p} \tag{54}$$

2.9.2 Planar wiggler

With the same assumption, one has:

$$\Delta l_{wp} \propto \frac{l^3}{N_w{}^2 p^2}(eB_0)^2\frac{\delta p}{p} \tag{55}$$

2.9.3 Helical wiggler

$$\Delta l_{wh} \propto 2\frac{l^3}{N_w{}^2 p^2}(eB_0)^2\frac{\delta p}{p} \tag{56}$$

for a wiggler with N_w period. Therefore,

$$\frac{\Delta l_c}{\Delta l_{wp}} = N_w{}^2 \tag{57}$$

which means that for similar values of the magnetic field, the chicane gives a compression proportional to the cube of the length, while when adding cells as a planar wiggler, the compression stays proportional to the cube of the length of the unit of cell, but is only proportional to the number of cells. Then the chicane is more efficient.

2.9.4 Alpha-magnet

Alpha-magnet is a generic term describing a range of achromatic mirrors [14]. The length of the particle trajectory, l_p, scales with momentum, p, as:

$$l_p \propto p^{\frac{1}{(1+n)}} \tag{58}$$

In the particular case of a quadrupolar field, n=1, and for small bunch momentum spread, one can approximate the gradient to:

$$G \simeq \frac{K^2(\frac{1}{p_0}\frac{dp}{dt})^2}{c^2}\frac{p_0}{4} \tag{59}$$

This system has to be used for bunches in which the particle momentum decreases monotonically from head to tail of the bunch contrary to the chicane and wiggler systems. With typical parameters of the CTF gun, we reach a 25 to 30 Tesla/m gradient. This implies a superconducting device.

2.9.5 Choice for the CTF

The choice of 3 dipoles with inverse polarity as a bunch compressor for CTF has been made with the following arguments:

- A system of three dipoles can be switched off if no compression is desired while the beam passes through the bunch compressor without seeing any field, contrary to the α-magnet compressor.
- The fields involved in those dipoles are weak, about 0.222 T at 20 MeV/c, versus superconducting quadrupoles needed for α-magnet. Accordingly, the size of the magnets can be very conservative, reducing the manufacturing and power supplies costs.
- The compression factor per unit of length is higher than the other methods. This characteristic is essential for the CTF line having a strong limitation in space.

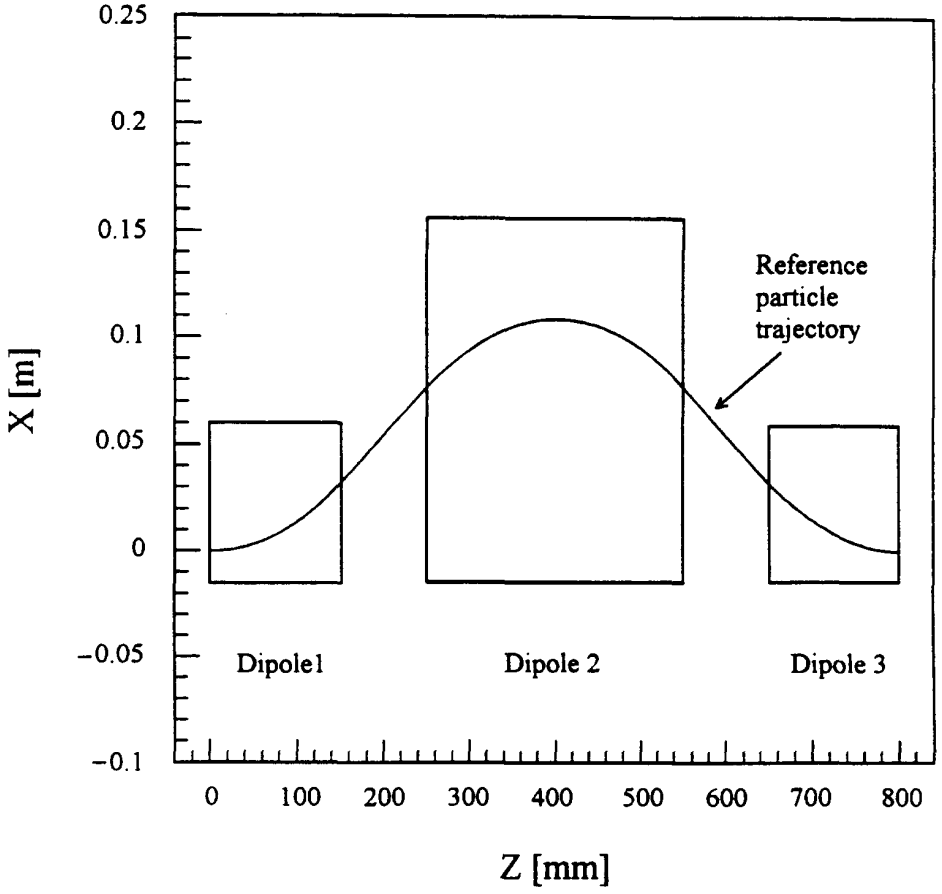

Figure 9: Central trajectory in the bunch compressor

3 Design of the CTF bunch compressor

3.1 Definition of the optics

As mentioned above, the bunch compressor chosen for the CTF is based on 3 dipoles with inverted polarity and full symmetry with respect to the central magnet axis. Table 2 summarises the characteristics discussed in the paragraph 2.5 for λ= 100 mm.

For a bunch compression at a maximum momentum of 20 MeV/c, the maximum magnetic field will be: B = 0.223 T. The good field region covers the maximum requirements. Under these conditions, the trajectory of the reference particle in the bunch compressor is plotted (Fig. 9). Uppsala University participated in the design of the bunch compressor and provided stimulating discussions [15].

	Central Magnet	End Magnets
good field region	170 mm	75 mm
effective length	300 mm	150 mm
aperture	70 mm	70 mm
Max. deflection angle	60°	30°
curvature radius ρ	300 mm	300 mm
Max. horizontal deviation D	138 mm	40 mm

Table 2: Magnet characteristics

3.2 Layout of simplified CTF line for simulations

Fig. 10 gives the layout of the optics from the RF gun up to the travelling wave section and including the bunch compression region. Figure 11 shows the layout of the CTF up to the first CLIC structure (TRS) as foreseen for 1995. It is composed of an RF gun (one and half cell S-band) at 4 MeV [16] with a photo-cathode (Cs_2Te); a booster structure (4 cells) providing a 7 MeV beam [17]; the bunch compressor, four quadrupoles to match the beam emittances to the entrance of LAS (LIL Accelerating Section). At the exit of LAS the beam energy is 68 MeV. A quadrupole triplet focuses the beam into the TRS (Transfer Structure). The rest of the line is not simulated with PARMELA code since it is not necessary for the design optimisation of the bunch compressor.

3.3 Optimisation of the phases.

Two phases are free parameters and are of great importance for the bunch compressor optimisation:

- Φ_{gun} is the phase when the center of the laser pulse hits the photo-cathode in respect with the 3 GHz RF voltage in the gun.
- $\Phi_{booster}$ is the phase of the 3 GHz RF voltage in the booster in respect with the same RF in the gun.

To achieve a compression with the magnetic chicane it is necessary to get a correlation between the phase and the energy of the particles as linear as possible. This correlation has to create bunches with momentum distribution that increases from head to tail. Otherwise the bunches would be lengthening instead of shortening. This correlation is obtained by an adjustment of the Φ_{gun} and $\Phi_{booster}$. The momentum and the momentum spread are plotted versus Φ_{gun} (Fig. 12 (a)) from PARMELA simulations. Two extrema appear for the momentum spread:

- $\Phi_{gun} = 25°$: the momentum spread is maximum and the correlation is rather good but the momentum is around 4.4 MeV/c.
- $\Phi_{gun} = 50°$: The momentum is maximum, 4.8 MeV/c, and the energy spread is minimum. As a consequence, the linear correlation is not good enough between the phase and the energy.

For these two extrema of Φ_{gun}, the momentum and the momentum spread are plotted versus $\Phi_{booster}$ (Fig. 12 (b),(c)). One can notice that at the maximum momentum, the momentum spread is close to its minimum.

A compromise has to be found between the maximum momentum spread and a minimum energy loss. According to the Figure 12, the following set of phases is chosen, for a 0 nC beam:

$$\phi_{gun} = 25°$$

$$\phi_{booster} = 264°$$

Giving,

$$\frac{\delta p}{p} = 3.8\%$$

3.4 Results from PARMELA simulations

Series of simulations are done to investigate the bunch compression for different beam charges: 0 nC, 1 nC, 3 nC, 5 nC and 10 nC. The simulations without space charge will allow to set up the element parameters to obtain a maximum transmission all through the CTF line (Fig. 11). This fitting is done by using the code TRANSPORT [8]. Nevertheless, TRANSPORT does not take into account the effect of the space charge, making the matching of the beam envelope more critical. To understand how evolves this effect, one can characterise this space charge force F_r in the simple case of a beam with a uniform particle density ρ_0 moving with the velocity v along the z-axis:

$$F_r = e(E_r - \frac{v}{c}B_\varphi) = \frac{2\pi e\rho_0}{\gamma^2}r$$

where

E_r is the radial electrical field from Coulomb's law $\nabla E = 4\pi\rho_0$ at the distance r from the beam axis,

B_φ is the azimuthal magnetic field derived from Ampere's law $\nabla \times B = \frac{4\pi}{c}\rho_0 v$.

Then the repelling electrostatic force is increasingly compensated by the magnetic force when γ increases.

The space charge effect has to be limited as much as possible because in the case of the bunch compression the distance between each particle becoming smaller, ρ_0 increases causing a growing repelling effect of this force. The induced beam divergence at the exit of the bunch compressor would be difficult to compensate needing strong quadrupoles. Two modifications were required to improve the compression process:

- Increase the bunch length at the input of the bunch compressor.
- Increase the beam energy.

By lengthening the electron bunch one decreases the particle density ρ_0, so is the space charge force. This is achieved by working on the natural length of the laser pulse, $\sigma_{max} = 16$ ps, hitting on the photo-cathode.

Additionally, the booster will increase γ up to 21.5 corresponding to β equal to 0.9989. The possibility to add another identical booster is still open. We rely on these two modifications to improve the transport of high charged beam toward the compressor system. After

compression, one has to minimise the distance between the exit of the bunch compressor and the entrance of LAS in which the bunch length will be frozen when the beam becomes completely ultra-relativistic.

3.4.1 Momentum spread function of the charge

The optimum $\delta p/p$=3.8% corresponds to a beam without space charge effects. However this value depends on the charge.

The momentum spread versus the charge is plotted, for $\phi_{gun} = 25°$ and $\phi_{booster} = 264°$:

- At the gun exit (Fig. 13 (a))
- At the booster exit (Fig. 13 (b))
- At the LAS exit (Fig. 13 (c))

At the exit of the booster (entrance of the bunch compressor), $\delta p/p$ drops from 3.84 % for 0 nC down to 3.55 % for 10 nC. The consequence will be a bunch compressor less efficient at high charge. However at the exit of LAS, the effect is inverted. $\delta p/p$ increases from 0.55% for 0 nC, up to 1 % for 10 nC.

Fortunately this value is still acceptable to keep a minimum beam loss through the CTF line.

3.4.2 Beam envelopes and emittances

The beam envelopes from the RF gun until the entrance of LAS are reported in the horizontal plane (Fig. 14) and in the vertical plane (Fig. 15) for the following initial charges:
0, 1, 3, 5, 10 nC.

These envelopes are restricted to the LAS input in order to analyse with better accuracy the region of the bunch compressor. On the same graphs, the aperture limitations of each element are drawn.
The only solenoid SNF350 allows to focus as good as possible the beam at the booster input. Its effect is clearly seen in the various plots. The optimised value found for the charge 10 nC is kept for all lower charges.
The settings of the four quadrupoles are optimised in order to have a minimum divergence at the entrance of LAS with a beam radius equal or less than 12 mm (iris aperture at the LAS input). As shown on Figures 14 and 15, these conditions are reached for a beam of 0 nC but not completely for a beam of 10 nC (particularly for the vertical plane).
Table 3 gives the input data which are independent of the charge and Table 4 those which are dependent of the charge. Table 5 and 6 give the output data.

The Appendix A gives the files which are used as input files for PARMELA simulations and the distribution of the magnetic field along LAS. The electric fields in the RF gun and the booster are described as ideal cosine functions. The number of macro particles is 300.

The results of the simulations show that a transmission of 100% is possible through the whole CTF line for a charge below 10 nC. For this latter value, the transmission drops to 87%.

The beam envelopes are now plotted from the RF gun until TRS in the horizontal plane (Fig. 16) and in the vertical plane (Fig. 17) for the same set of initial charges. One can see that the main losses, for 10 nC, are due to LAS aperture, mainly in the vertical plane.

Laser pulse length:	
σ_L [ps]	8.
σ_{Lmax} [ps]	16.
Laser pulse transverse size:	
σ_r [mm]	3.
σ_{rmax} [mm]	5.
Φ_{gun} [deg]	25.
$\Phi_{booster}$ [deg]	264
SNF350 [T]	0.24
QD410 [T/m]	0.37
QF415 [T/m]	- 0.47
QD420 [T/m]	0.24

Table 3: Input data (independent of the charge)

Charge [nC]	Field chicane [T]	Q1 [T/m]	Q2 [T/m]	Q3 [T/m]	Q4 [T/m]	Field LAS [T]	Trans-mission [%]
0	.050	.54	-.34	.34	-.37	0.	100
1	.054	.67	-.23	.34	-.49	.05	100
3	.056	.70	-.19	.34	-.59	.1	100
5	.058	.44	.07	.34	-.67	.1	100
10	.067	.68	-.24	.39	-.57	.1	87

Table 4: Input data and transmission results (charge-dependent)

Momentum: P [MeV/c]	
At the exit of the gun:	4.5
At the exit of the booster:	10.67
At the entrance of TRS:	68.3
Momentum spread: $\delta p/p$ [%]	
At the exit of the gun:	2.5
At the exit of the booster:	3.8
At the entrance of TRS :	0.56
RMS transverse sizes [mm]	
At the exit of the gun:	x=y=3.6
At the exit of the booster:	x=y=3.0
At the exit of the bunch compressor:	x=2.8, y=1.8
At the entrance of TRS :	x=0.4, y=0.8
RMS transverse divergences [mrad]	
At the exit of the gun:	x'=y'=22.5
At the exit of the booster:	x'=y'=2.4
At the exit of the bunch compressor:	x'=2.4, y'=1.6
At the entrance of TRS :	x'=0.9, y'=0.7
RMS normalized beam emittances ϵ [mm.mrad]	
At the exit of the gun:	ϵ_H=ϵ_V=44.
At the exit of the booster:	ϵ_H=ϵ_V=53.
At the exit of the bunch compressor:	ϵ_H=ϵ_V=61.
At the entrance of TRS :	ϵ_H=57., ϵ_V=63.

Table 5: Output data for 0 nC

Momentum: P [MeV/c]	
At the exit of the gun:	4.5
At the exit of the booster:	10.8
At the exit of the bunch compressor:	10.8
At the entrance of TRS:	64.7
Momentum spread: $\delta p/p$ [%]	
At the exit of the gun:	1.6
At the exit of the booster:	3.6
At the exit of the bunch compressor:	2.6
At the entrance of TRS :	1.1
RMS transverse sizes [mm]	
At the exit of the gun:	x=y=4.5
At the exit of the booster:	x=y=4.7
At the exit of the bunch compressor:	x=4.5, y=1.0
At the entrance of TRS :	x=1.4, y=1.3
RMS transverse divergences [mrad]	
At the exit of the gun:	x'=y'=31.0
At the exit of the booster:	x'=y'=1.0
At the exit of the bunch compressor:	x'=2.0, y'=6.8
At the entrance of TRS :	x'=0.9, y'=1.6
RMS normalized beam emittances ϵ [mm.mrad]	
At the exit of the gun:	$\epsilon_H=\epsilon_V=64.$
At the exit of the booster:	$\epsilon_H=\epsilon_V=70.$
At the exit of the bunch compressor:	$\epsilon_H=132.0$, $\epsilon_V=60.0$
At the entrance of TRS :	$\epsilon_H=167.$, $\epsilon_V=190.$

Table 6: Output data for 10 nC

However, 100% of particles can be focused correctly in the TRS for all charges which is one of the goals of this study.

Finally, the transverse phase spaces are characterised at 0 nC (Fig. 18) and at 10 nC (Fig. 19) at three different critical places of the CTF.

- At 0 nC, only the RF fields and the magnetic fields contribute to this particular distribution (butterfly shape). After the bunch compressor the horizontal beam dimensions are increased, due to the fact that the horizontal dispersion is not completely cancelled. Although both transverse planes are not completely similar, with the proposed optic settings (Table 4), it has been possible to obtain the same emittances for the horizontal and vertical planes at the exit of the bunch compressor (Table 5). In TRS, the butterfly shape is recovered in both planes and with acceptable values.

- At 10 nC, the space charge effects are predominant and with a minimum divergence at the bunch compressor input in both planes, there is a tremendous effect for the vertical divergence at the bunch compressor exit. The consequence is that the quadruplet cannot compensate this effect before entering in LAS and therefore 13% losses are produced in LAS. However at TRS, both transverse phase spaces have decent values for such high charges.

3.4.3 Longitudinal phase space

In order to optimise the bunch compressor, the longitudinal phase space is analysed in four particular places of the CTF (Fig. 11):

- At the bunch compressor input: element 17.
- At the bunch compressor output: element 23.
- At the entrance of LAS: element 37.
- At the entrance of TRS: element 61.

The longitudinal phase spaces are plotted at the 4 elements mentioned above:

- elements 17, 23, 37

  0 nC (Fig. 20)
  1 nC (Fig. 21)
  3 nC (Fig. 22)
  5 nC (Fig. 23)
  10 nC (Fig. 24)

- element 61

  0, 1, 3 nC (Fig. 25)
  5, 10 nC (Fig. 26)

Charge [nC]	α [deg]	$\Delta\Phi_{17}$ [deg]	$\Delta\Phi_{23}$ (FWHH)[deg]	$\Delta\Phi_{61}$ (FWHH)[deg]	compression rate 17/23	compression rate 17/61
0	13.	11.25	1.5	1.5	7.5	7.5
1	14.	11.25	1.5	1.5	7.5.	7.5
3	14.5	12.	3.	3.	4.	4.
5	15.	13.	3.2	5.	4.	2.6
10	17.5	13.	3.2	7.	4.	1.8

Table 7: Simulation results in phase

Charge [nC]	α [deg]	σ_{17RMS} [mm]	σ_{23RMS} [mm]	σ_{61RMS} [mm]	compression rate 17/23	compression rate 17/61
0	13.	1.04	.25	.23	4.2	4.5
1	14.	1.07	.25	.25	4.3	4.3
3	14.5	1.13	.32	.42	3.5	2.7
5	15.	1.18	.38	.51	3.1	2.3
10	17.5	1.3	.35	.68	3.7	2.

Table 8: Simulation results in RMS

For each Figure, the longitudinal phase space is given with the coordinates $(\gamma\beta_z, \phi)$ and a corresponding histogram is given with the coordinates (number of particle, ϕ)

In the table 7, the bunch lengths are reported in $\Delta\phi$ (degrees) according to the histogram plots (Fig. 20 to 26).

In the Table 8, the same bunch lengths are reported in σ (mm) according to the PARMELA output.

The fact that the bunch compressor factor is not the same according to the tables 7 and 8 (mainly at low charge) is due to the sharp edge of the distribution in phase. Therefore the σ value does not represents correctly this non-symmetric distribution.

- At 0 nC: An optimum compression is calculated without space charge effect. The compression rate (Table 7) obtained at the element 23 is 7.5. The shape of the bunch is slightly curved due to the sine shape of the RF wave. Then the compression gives to a "moon-shape" in the longitudinal phase space reducing the compression rate, because the compression process is based on a perfect elliptical longitudinal phase space (Fig. 1). It is impossible to have the ideal straight ellipse before compression. Additionally the simulations show that most of the particles lay in the front of the bunch. Then one has to take into account the head of the bunch as reference for the compression, taking care to compress enough to place all the front particles almost in phase with the reference particle. The position of the bunch tail is of less importance.

  The transmission through all the CTF line is 100%.

  The bunch length is conserved until the entrance of TRS. Its value is 1.4 ps (FWHH) or 0.83 ps (RMS) or 1.5 degree (FWHH).

- With charge: The optics before the bunch compressor stay the same when the charge is varied. Only the four quadrupoles would have to compensate the very strong divergence of the beam after compression. The settings of the quadrupoles are changed for each different charge in order to get a maximum transmission (Table 4). The field in the dipoles is increased with the charge.

  The space charge forces introduce a longitudinal emittance growth. Figure 27 characterises its effect on a compressed beam at 3 nC. The phenomenon is the following: The particles in the front of the beam are accelerated by the repulsive force from the other particles of the beam, while the particles in the tail are decelerated for the same reason. Both phenomena tend to rotate the phase space clockwise (see evolution of the scatter plots (a) in Fig. 20 to 24). Then, for a non-relativistic bunch in the drift before the bunch compressor these phenomena will first reduce the momentum spread of the beam. After compression when the correlation almost disappeared the momentum spread will grow (see scatter plots (c) in Figures 20 to 24). Figure 13 shows the evolution of the momentum spread.

The σ of the compressed bunch length at 5 nC, is greater than at 10 nC (Table 8). This is explained by a not completely optimised angle α for 5 nC.

Although the bunch length is in the range of 5° *at the entrance of LAS (Fig. 24 (c)), it becomes of the order of* 10° *at the TRS input (Fig. 26 (b)). It is not yet clarified if it is a physical phenomenon or simply a numerical effect from PARMELA. This bunch lengthening appears when a magnetic field is superimposed on the accelerating structure (LAS).*

Further simulations are done in order to understand this effect and find a correct setting which allows to keep a short bunch with high charge at TRS input.

3.4.4 Other improvements

- For a given bunch length, the compressed bunch length can be minimised by increasing $\delta p/p$ (see 2.4). However, the opposite effect occurs when the charge increases (Fig. 13). At the exit of the gun and at the exit of the booster $\delta p/p$ gets smaller, in a range of 38% and 7% respectively, inducing a larger phase spread, Φ_{int}, after compression. A higher momentum spread is obtained by changing ϕ_{gun} and $\phi_{booster}$. Then it remains to optimise the phase of LAS to improve the compression.

- A higher electric field in the gun and in the booster would improve the overall scheme. The "moon-shape" in the phase space at low charge would be reduced. Therefore the compression rate would be improved.

4 CTF line 1995

4.1 New layout

As already mentioned, one of the CTF objectives is to produce short and intense electron pulses in order to check the generation of 30 GHz RF power.

Another objective is to check that an acceleration with such RF power is possible with gradients equal to 80 MV/m.

The complete layout of the CTF as foreseen for 1995 is given (Fig. 28).

The 30 GHz RF power generated in TRS is sent to the CAS (CLIC Accelerating Structure).

From the simulations, one can expect to produce 60 MW peak in TRS, with the compressed bunches, corresponding to an electric field of 113 MV/m in TRS. Taking into account the efficiency factor , it would be possible to get 80 MV/m in the CAS.

Fig. 29 shows the mechanical layout of the bunch compressor region.

It is now designed and mechanical pieces are ordered according to this configuration.

4.2 Bunch compressor off

Up to now, design and simulations have been presented assuming that the bunch compressor was working continuously. However, the option to accelerate beam in LAS without any compression is strongly recommended.

For the set-up of the CTF, at least at low energy and for specific studies, in single bunch and with a train of bunches, one should transport the beam through the bunch compressor system without any loss when this latter is off.

PARMELA simulations have been performed under this hypothesis.

Fig 30 and 31 show respectively the horizontal and vertical beam envelopes from the RF gun up to TRS input.

According to the simulations, the 1995 CTF line could work without the bunch compressor.

4.3 Spectrometer line

In order to measure some beam characteristics, a spectrometer line is implemented (see 2.6 and Fig. 29). A scintillator screen will be installed in the line and the optimised position is derived from Fig. 7. The vacuum chamber is 60 mm in the horizontal plane. The aperture of the Faraday cup is 35 mm. In order to transport all the beam to the Faraday cup, the simulations with TRANSPORT code give a distance for a screen, followed by a Faraday cup, of 700 mm downstream the exit of the first dipole.

The beam characteristics at this point and at 0 nC are:

x_1 =34.6 mm
x'_1 =22.3 mrad
y_1 =1.4 mm
y'_1 =2.3 mrad

These values are optimised for a good matching in the Faraday cup and a good resolution as spectrometer line.

4.4 Proposed settings for the 1995 CTF

(At low charges)

Laser	pulse length	:	19 ps (FWHH)
	energy	:	0.2 mJ
RF gun	ϕ_{gun}	:	25°
	$\vec{E}_{gun}$	:	100 MV/m
	RF power	:	6.0 MW
SNF350	B	:	0.24 T
	I	:	69. A
Booster	$\phi_{booster}$	:	264°
	$\vec{E}_{booster}$	:	70 MV/m
	RF power	:	8.3 MW
Bunch compressor	α	:	14.5°
	$\vec{B}$	:	0.056 T
	I_1	:	22.6 A
	I_2	:	22.6 A
Quadruplet	G_1	:	0.70 T/m
	G_2	:	-0.19 T/m
	G_3	:	0.34 T/m
	G_4	:	-0.59 T/m
	I_1	:	2.8 A
	I_2	:	0.8 A
	I_3	:	1.4 A
	I_4	:	2.4 A
LAS	ϕ_{LAS}	:	350°
	$\vec{E}_{LAS}$	:	17 MV/m
	RF power	:	30 MW
	$\vec{B}_{LAS}$	:	0.1 T
Triplet	G_1	:	1. T/m
	G_2	:	-2.3 T/m
	G_3	:	1.45 T/m
	I_1	:	4. A
	I_2	:	9.2 A
	I_3	:	5.8 A
TRS	e^- pulse length	:	
	σ_z	:	0.42 mm
	σ_t	:	1.4 ps
	Δt (FWHH)	:	3.3 ps
	charge Q	:	3 nC
	$\vec{E}_{dec}$	:	113 MV/m

5 Conclusion

This note is the first step in the design of the bunch compressor for the CTF. The sensitivity of the system to the geometric aberrations and chromatic effects is in progress. The main objective to produce and accelerate single bunches of 10 nC and $\sigma_t \leqslant 3$ ps is reached.

Under these conditions, the total transmission is close to 90% until the CLIC structure TRS. In consequence and based on these simulation results, the mechanical design of the bunch compressor has been finalised and the order has been placed. It is foreseen to receive the entire system before the end of the year in order to do the magnetic measurements and install the bunch compressor in the CTF at the beginning of 1995.

6 Acknowledgements

A number of people made very useful comments and suggestions to this study. In particular the CTF beam dynamics working group: H. Braun, J.P. Delahaye, G. Guignard, J.H.B. Madsen, A. Riche. B. Mouton and W. Remmer provided a great help for the improvements of the code PARMELA. D. Reistad (Uppsala University) gave a valuable contribution to the design of the bunch compressor.

Appendices

A PARMELA input files

A.1 PARMELA input listing

The following input file has been used for a 0 nC beam. The cards used are fully described in [6].

```
TITLE
Gun 100 MV/m, Booster 70 MV/m, Optics for 1995
RUN /NO= 6 / 1 /FREQ= 2998.55 MHz /Z0= 0. CM
/E0= 2.0e-12 MeV / 1
OUTPUT 6
FOCLAL /ZMIN= 342.3 /ZMAX= 912.3 /DZZ= 10.
/NPCHB= 58 /COEFF= 1.0 /OPT= 0
bzfield
CELL /L=2.5 /APER=1.0 /IOUT=1 /phi0= 0.0 /E0=63.657
/CELL=1 /DWTMAX=1 /SYM= -1 /CFREQ=0 /CTYPE=1
/BZ=0. /NFC=1 /VV=1 /NECR=1
1.5708
CELL /L=2.5 /APER=1.5 /IOUT=1 /phi0= 180.0 /E0=63.657
/CELL=2 /DWTMAX=2 /SYM= 1 /CFREQ=0 /CTYPE=1
/BZ=0. /NFC=1 /VV=1 /NECR=1
1.5708
CELL /L=5.0 /APER=1.5 /IOUT=1 /phi0= 180.0 /E0=56.586
/CELL=3 /DWTMAX=2 /SYM= -1 /CFREQ=0 /CTYPE=1
/BZ=0. /NFC=2 /VV=1 /NECR=2
1.5708,0.5236
DRIFT /L= 2.33 /APER= 1.5 /IOUT=1
SOLENOID /L= 5.34 /A=1.5 /IOUT=1 /B= 2400. ;SNF 350
CELL /L=5.0 /APER=1.5 /IOUT=1 /phi0= 260.0 /E0=39.61
/CELL=4 /DWTMAX=3 /SYM= 1 /CFREQ=0 /CTYPE=1
/BZ=0. /NFC=2 /VV=1 /NECR=2
1.5708,0.5236
CELL /L=2.5 /APER=1.5 /IOUT=1 /phi0= 260.0 /E0=44.56
/CELL=5 /DWTMAX=3 /SYM= -1 /CFREQ=0 /CTYPE=1
/BZ=0. /NFC=1 /VV=1 /NECR=1
1.5708
CELL /L=5.0 /APER=1.5 /IOUT=1 /phi0= 80.0 /E0=44.56
/CELL=6 /DWTMAX=3 /SYM=0 /CFREQ=0 /CTYPE=1
/BZ=0. /NFC=1 /VV=1 /NECR=1
1.5708
CELL /L=5.0 /APER=1.5 /IOUT=1 /phi0= 260.0 /E0=44.56
/CELL=7 /DWTMAX=3 /SYM=0 /CFREQ=0 /CTYPE=1
/BZ=0. /NFC=1 /VV=1 /NECR=1
1.5708
CELL /L=2.5 /APER=1.5 /IOUT=1 /phi0= 80.0 /E0=44.56
/CELL=8 /DWTMAX=3 /SYM= 1 /CFREQ=0 /CTYPE=1
/BZ=0. /NFC=1 /VV=1 /NECR=1
1.5708
CELL /L=5.0 /APER=1.5 /IOUT=1 /phi0= 80.0 /E0=39.61
/CELL=9 /DWTMAX=3 /SYM= -1 /CFREQ=0 /CTYPE=1
/BZ=0. /NFC=2 /VV=1 /NECR=2
1.5708,0.5236
DRIFT /L= 137.0 /APER= 2.0 /IOUT= 1
BEND /L=15.130 /A=20.0 /IOUT=1 /WR=10.102 /AL=13.00
```

```
/B1=0.0 /B2=13.00 /PSI1=0.0 /PSI2=0.0 /R1=0.0 /R2=0.0
DRIFT /L= 10.0 /APER= 2.0 /IOUT= 1
BEND /L=30.26 /A=20.0 /IOUT=1 /WR=10.102 /AL=-26.00
/B1=-13.00 /B2=-13.00 /PSI1=0.0 /PSI2=0.0 /R1=0.0
/R2=0.0
DRIFT /L= 10.0 /APER= 2.0 /IOUT= 1
BEND /L=15.13 /A=20.0 /IOUT=1 /WR=10.102 /AL=13.00
/B1=13.00 /B2=0.00 /PSI1=0.0 /PSI2=0.0 /R1=0.0 /R2=0.0
DRIFT /L= 9.50 /APER= 2.0 /IOUT= 1
QUAD /L= 10.4 /APER= 2.9 /IOUT= 1 /BP= 54.0
DRIFT /L= 9.00 /APER= 2.0 /IOUT= 1
QUAD /L= 10.4 /APER= 2.9 /IOUT= 1 /BP= -34.5
DRIFT /L= 9.00 /APER= 2.0 /IOUT= 1
QUAD /L= 10.4 /APER= 2.9 /IOUT= 1 /BP= 34.5
DRIFT /L= 9.00 /APER= 2.0 /IOUT= 1
QUAD /L= 10.4 /APER= 2.9 /IOUT= 1 /BP= -37.0
DRIFT /L= 4.50 /APER= 2.0 /IOUT= 1
DRIFT /L= 74.10 /APER= 2.0 /IOUT= 1
CELL /L=3.3333 /APER=1.25 /IOUT=1 /PHI0= 20.
/E0=8.6054 /NC=10 /DWT=2. /SYM=1 /CFREQ= 2998.55
/CTYPE=1 /BZ=0. /NFC=14 /COS=1 /NECR=14
0.1704634E+01,0.3405747E+00,-.1342430E+00,-.3698516E-01,
0.1405716E-01,0.3110588E-02,-.3895104E-03,-.4738850E-04,
0.2688355E-05,0.3202221E-07,0.9270728E-08,0.6640441E-07,
-.9901883E-07,-.7171031E-07
TRWAVE /L = 1.6667 /APER = 1.250 /IOUT = 1
/PHI = 290.00 /E0 = 13.6 /NC = 11 /DWTMAX = 1.
/FREQ = 2998.55 /GAP = 0. /NMIN = -5 /NMAX = 5
/PSHIT = .6667 /NW = 138 /NPRINT = 0
/Z1 = 129.3 /Z2 = 138.1 /R1 = 0. /R2 = .5 /DPHI = 800.
TRWAVE 3.3333 1.250 1 290.00 13.6 11 1. 2998.55 0.0
TRWAVE 3.3333 1.250 0 290.00 13.6 11 1. 2998.55 0.0
TRWAVE 3.3333 1.250 0 290.00 13.6 11 1. 2998.55 0.0
TRWAVE 3.3333 1.250 0 290.00 13.6 11 1. 2998.55 0.0
TRWAVE 3.3333 1.250 0 290.00 13.6 11 1. 2998.55 0.0
TRWAVE 3.3333 1.250 0 290.00 13.6 11 1. 2998.55 0.0
TRWAVE 3.3333 1.250 0 290.00 13.6 11 1. 2998.55 0.0
TRWAVE 3.3333 1.250 0 290.00 13.6 11 1. 2998.55 0.0
TRWAVE 3.3333 1.250 0 290.00 13.6 11 1. 2998.55 0.0
TRWAVE 3.3333 1.250 0 290.00 13.6 11 1. 2998.55 0.0
```

⋮

120×(TRWAVE 3.3333 1.250 0 290.00 13.6 11 1. 2998.55 0.0)

⋮

```
TRWAVE 3.3333 0.900 1 290.00 13.6 11 1. 2998.55 0.0
TRWAVE 3.3333 0.900 0 290.00 13.6 11 1. 2998.55 0.0
TRWAVE 3.3333 0.900 0 290.00 13.6 11 1. 2998.55 0.0
TRWAVE 3.3333 0.900 0 290.00 13.6 11 1. 2998.55 0.0
TRWAVE 3.3333 0.900 0 290.00 13.6 11 1. 2998.55 0.0
TRWAVE 3.3333 0.900 1 290.00 13.6 11 1. 2998.55 0.0
TRWAVE 1.6667 0.900 1 290.00 13.6 11 1. 2998.55 0.0
DRIFT /L= 55.4 /APER= 2.0 /IOUT= 1
QUAD /L= 20.0 /APER= 2.0 /IOUT= 1 /GR= 105.25
DRIFT /L= 9.80 /APER= 2.0 /IOUT= 1
```

```
QUAD /L= 20.0 /APER= 2.0 /IOUT= 1 /GR= -233.
DRIFT /L= 9.80 /APER= 2.0 /IOUT= 1
QUAD /L= 20.0 /APER= 2.0 /IOUT= 1 /GR= 145.35
DRIFT /L=200.0 /APER= 2.0 /IOUT= 1
DRIFT /L= 35. /APER= 00.2 /IOUT= 1 ; TRS
ZOUT
INPUT 10 /NP=299 /SIGT= 8. /TMAX= 16. /SIGR= 0.3
/RMAX= 0.5 /W0= 2.0e-12 /DW0= 0 /DWT= 2. /RAN= 1
SCHEFF /Q=-6.25e10 /LR= 0.6 /LZ= 0.6 /NR= 10 /NZ= 20
/NIP= 0 /PL= 0. /OPT= 0 /FRM= 10. /RWAL= 0
/POINT= -.5
START /PHIO= 25. /DWT= 2. /NST= 100000 /NSC= 0
/NOUT= 0
END
```

A.2 Magnetic field along LAS

A magnetic field along LAS, represented by the TRWAVE cards, can be switched on and off by the use of a FOCLAL card. This card calls the file 'bzfield' given below. Additionally, the value of this field can be modulated by a factor 'COEFF' in FOCLAL.

```
$ champ chp=
10.0,
50.0,
200.0,
400.0,
600.0,
800.0,
1000.0,
1000.0,
1000.0,
1000.0,
1000.0,
1000.0,
1000.0,
1000.0,
1000.0,
1000.0,
1000.0,
1000.0,
1000.0,
1000.0,
1000.0,
1000.0,
1000.0,
1000.0,
1000.0,
1000.0,
1000.0,
1000.0,
1000.0,
1000.0,
1000.0,
1000.0,
1000.0,
1000.0,
1000.0,
1000.0,
```

```
1000.0,
1000.0,
1000.0,
1000.0,
1000.0,
1000.0,
1000.0,
1000.0,
1000.0,
1000.0,
1000.0,
1000.0,
1000.0,
1000.0,
1000.0,
1000.0,
1000.0,
1000.0,
1000.0,
1000.0,
1000.0,
800.0,
600.0,
400.0,
200.0,
50.0,
10.0,
$ end
```

B Graphics

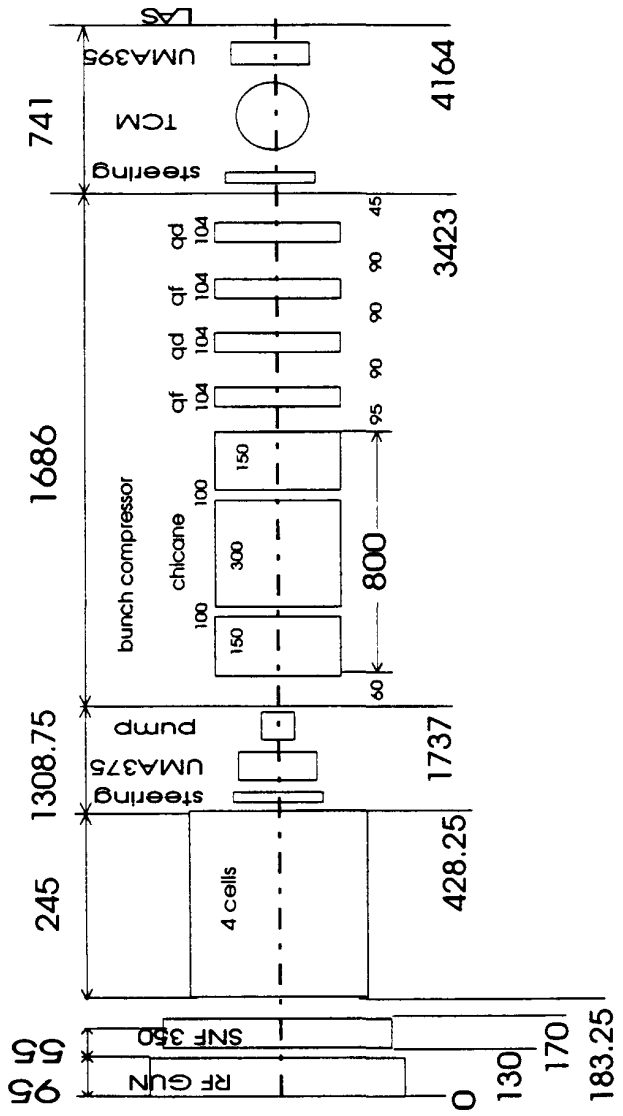

Figure 10: CTF optics in the bunch compressor region.
(Electric or magnetic lengths are effective lengths)
[Dimension in mm]

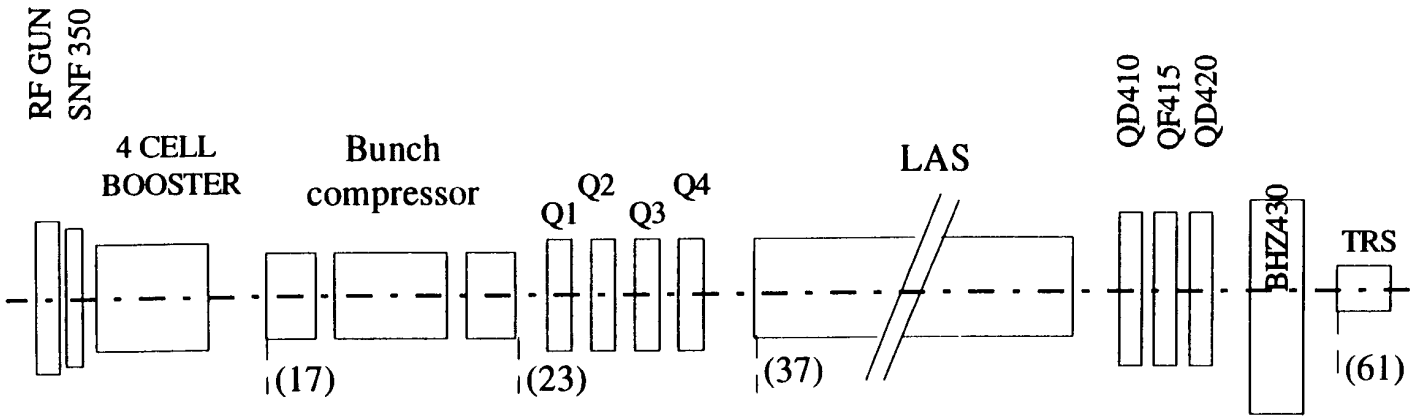

Figure 11: Simplified CTF layout for simulations

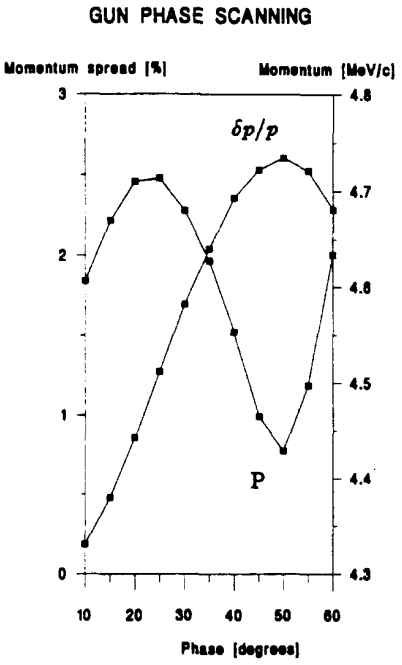

(a)

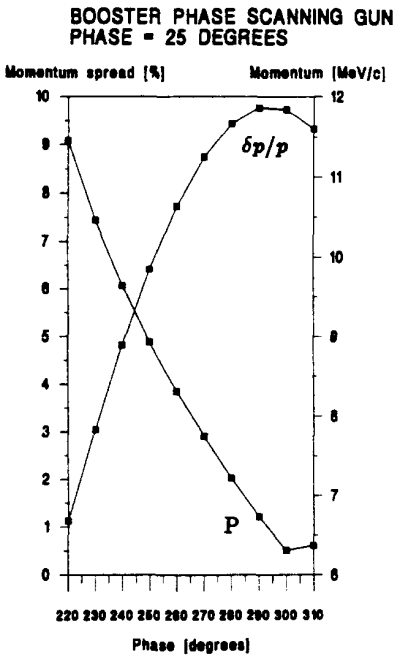

(b)

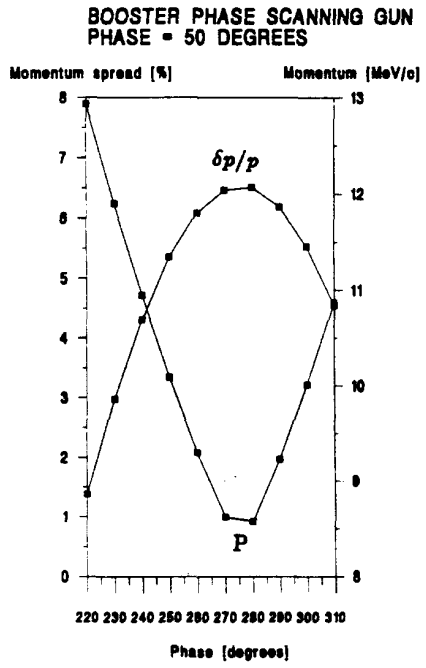

(c)

Figure 12: Phase scannings at 0 nC.

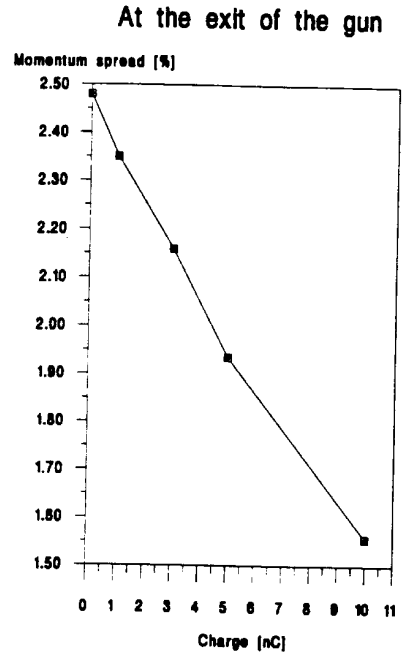

(a)

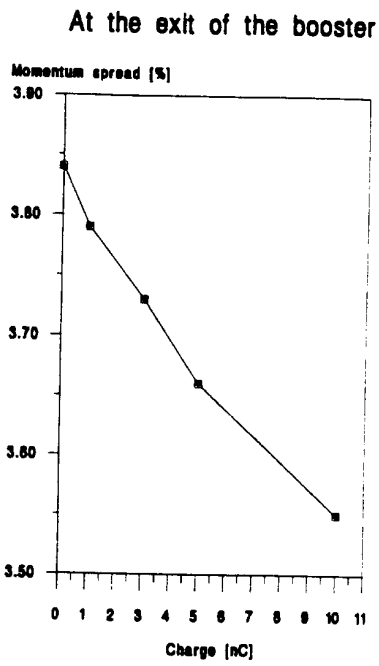

(b)

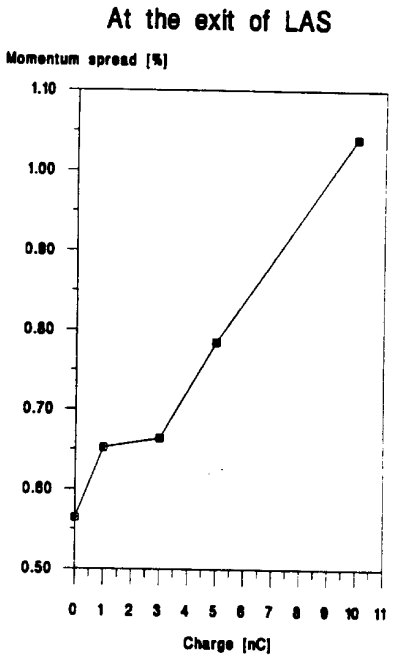

(c)

Figure 13: Momentum spread function of the charge

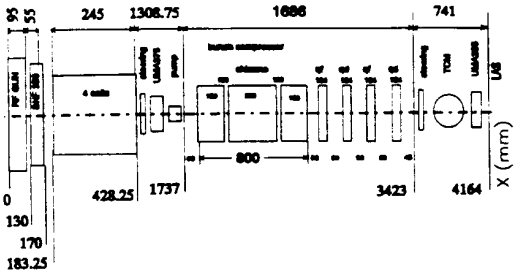

(a) Fig. 10

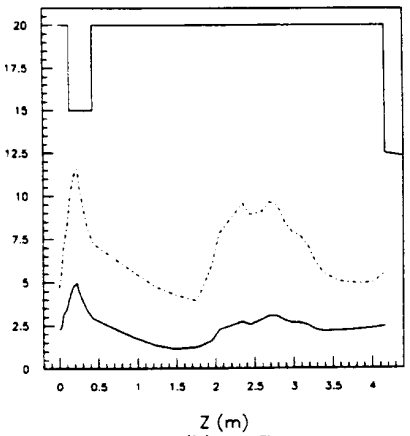

(b) 0 nC

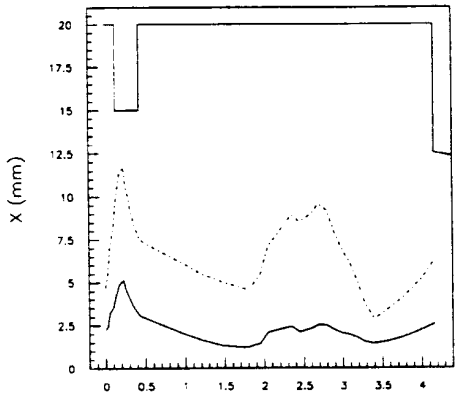

(c) 1 nC

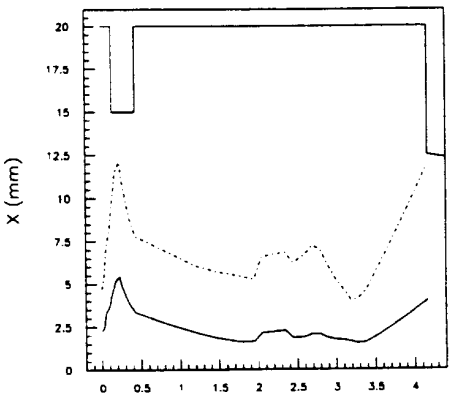

(d) 3 nC

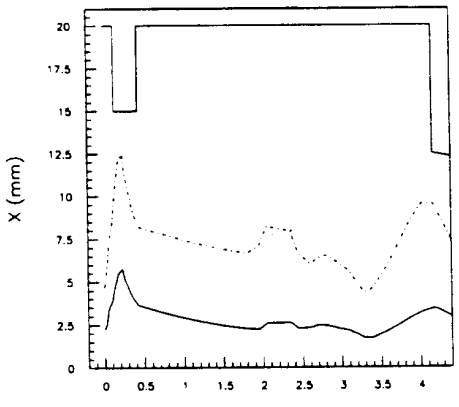

(e) 5 nC

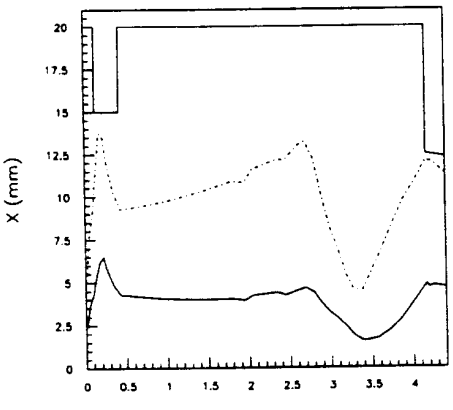

(f) 10 nC

Figure 14: Horizontal beam envelopes in the bunch compressor region. (...): 100% particles. (-): rms value.

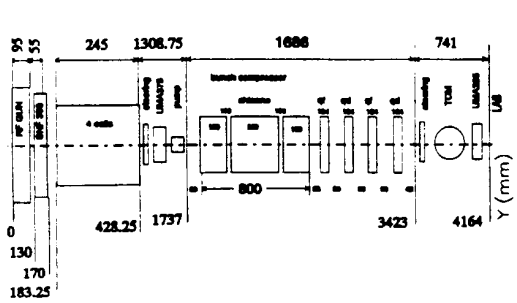

(a) 10

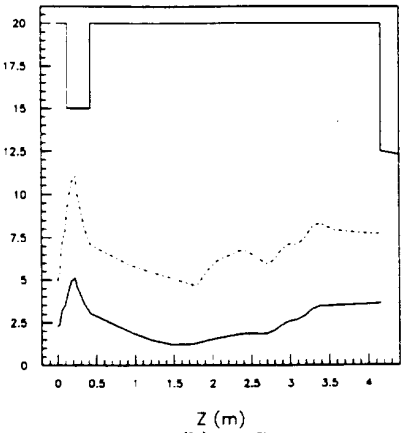

(b) 0 nC

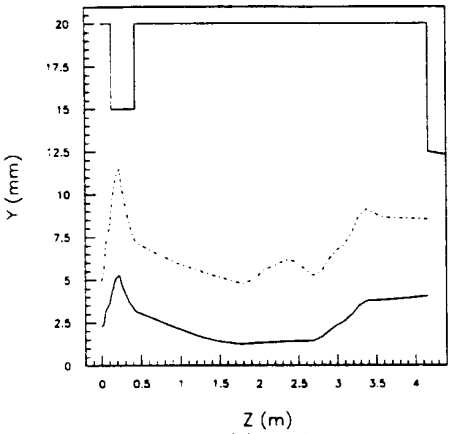

(c) 1 nC

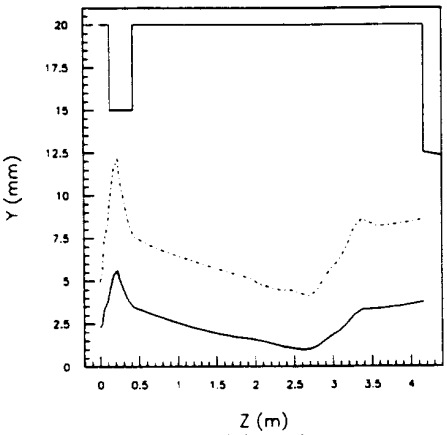

(d) 3 nC

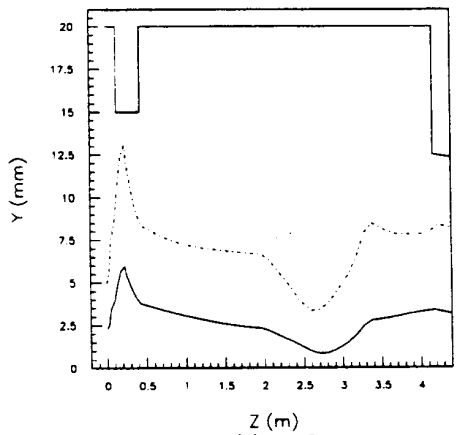

(e) 5 nC

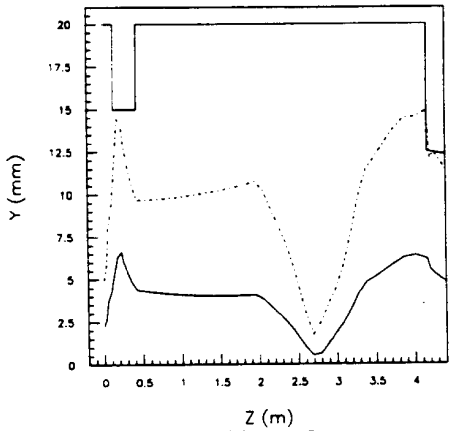

(f) 10 nC

Figure 15: Vertical beam envelopes in the bunch compressor region. (...): 100% particles. (-): rms value.

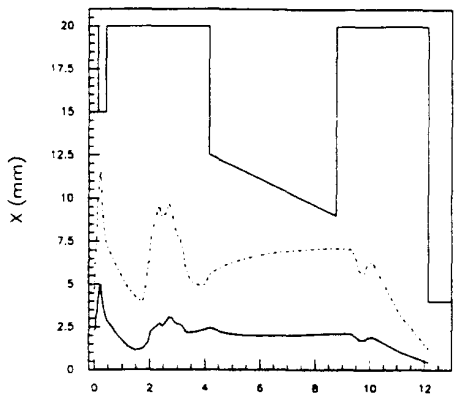

(a) 0nC

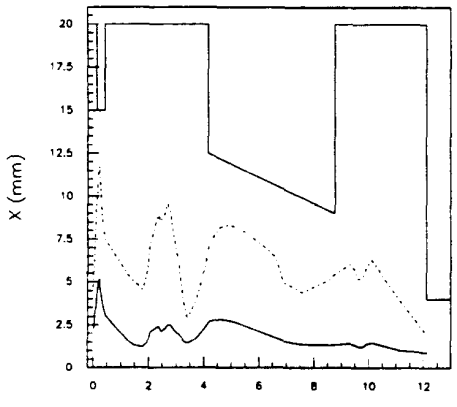

(b) 1 nC

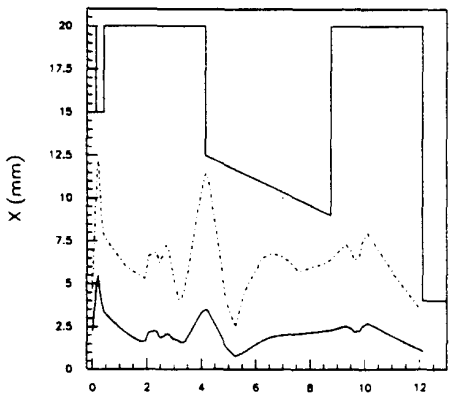

(c) 3 nC

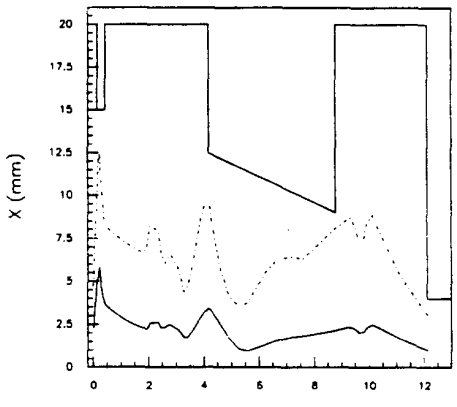

(d) 5 nC

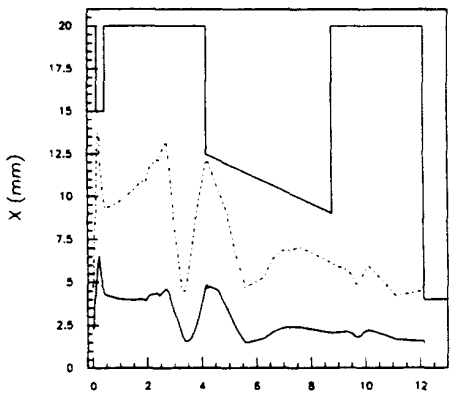

(e) 10 nC

Figure 16: Horizontal beam envelopes for the simplified CTF line. (...): 100% particles. (-): rms value.

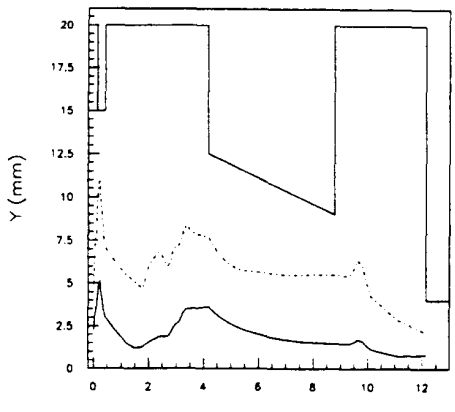

(a) 0 nC

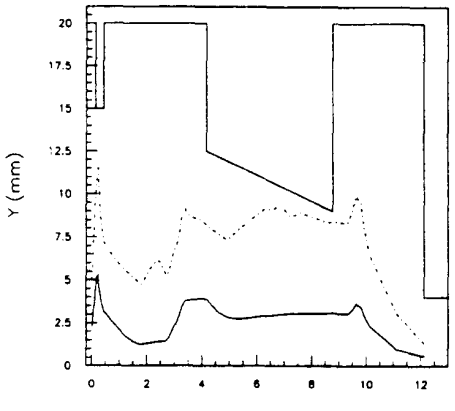

(b) 1 nC

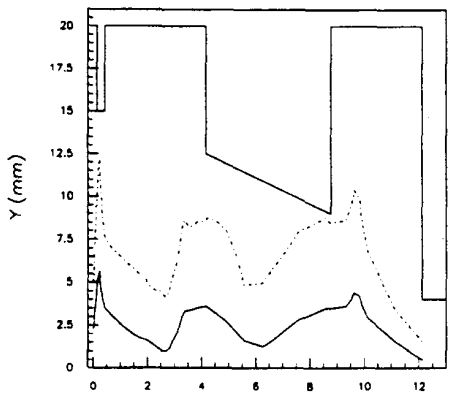

(c) 3 nC

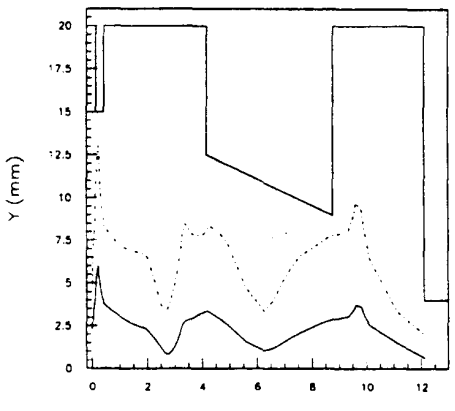

(d) 5 nC

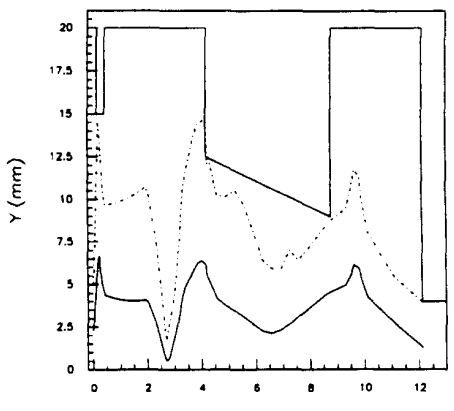

(e) 10nC

Figure 17: Vertical beam envelopes for the simplified CTF line. (...): 100% particles. (-): rms value.

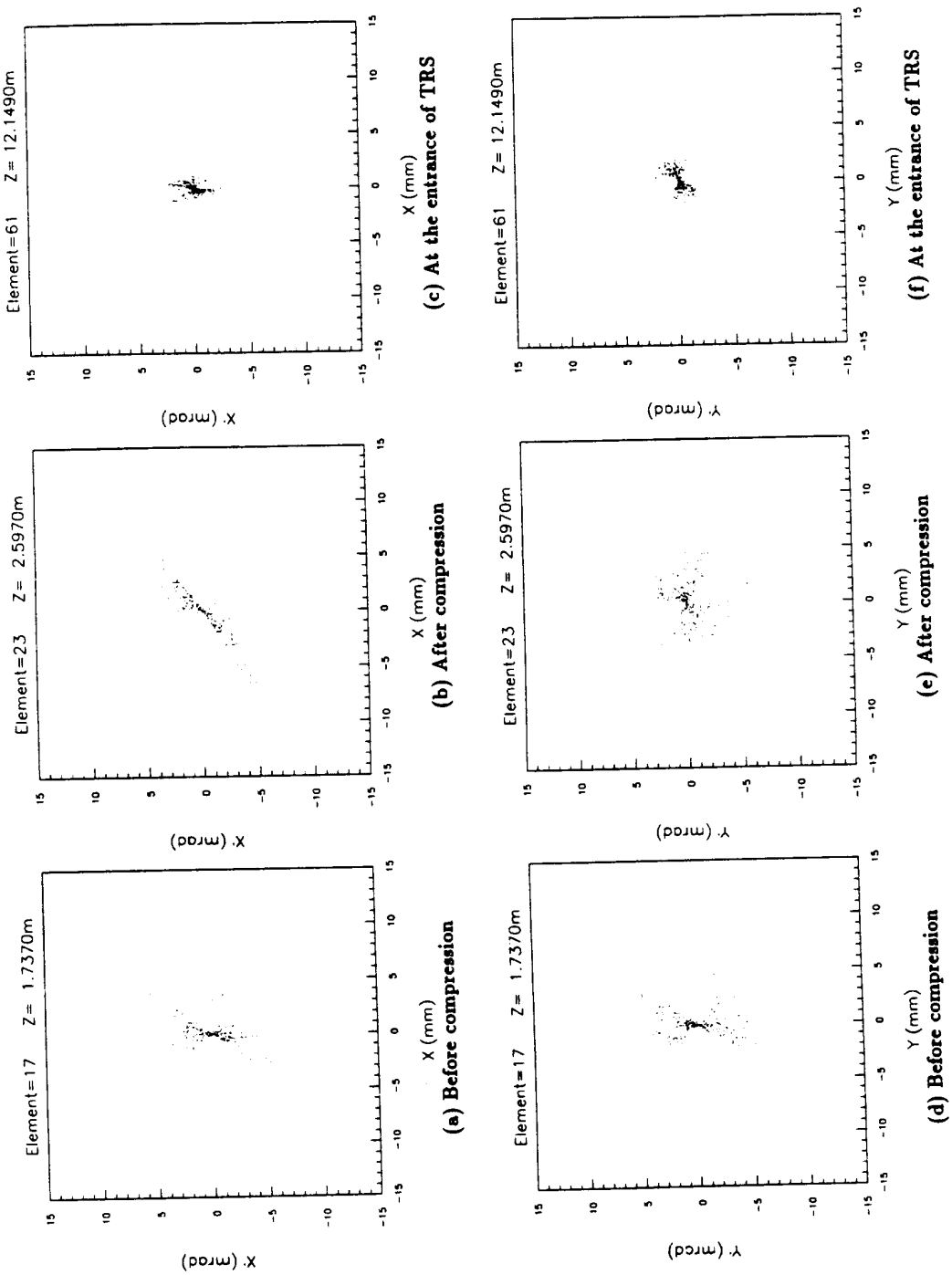

Figure 18: (x,x') and (y,y') phase space evolutions through the CTF line for a 0 nC beam.

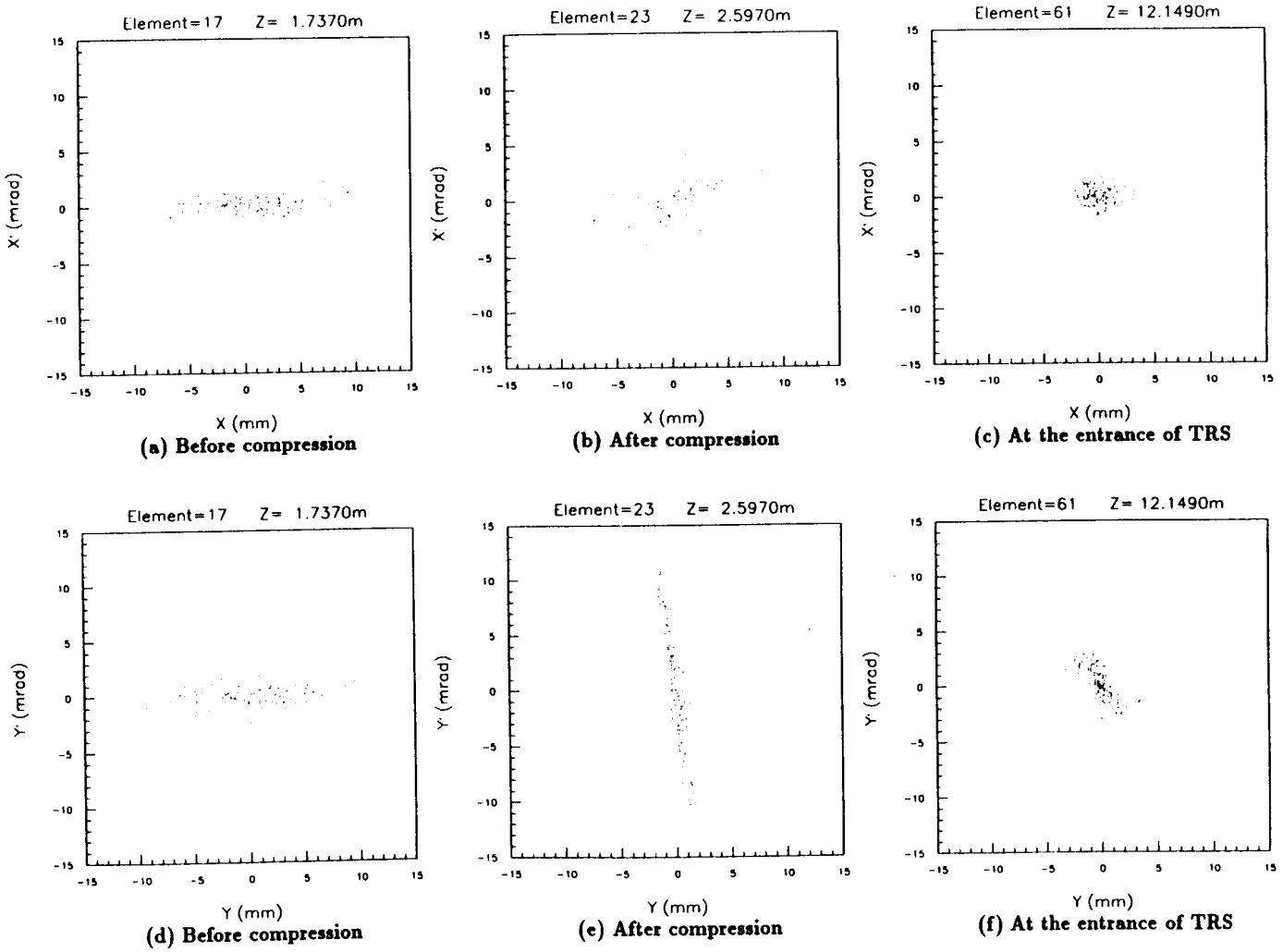

Figure 19: (x,x') and (y,y') phase space evolutions through the CTF line for a 10 nC beam.

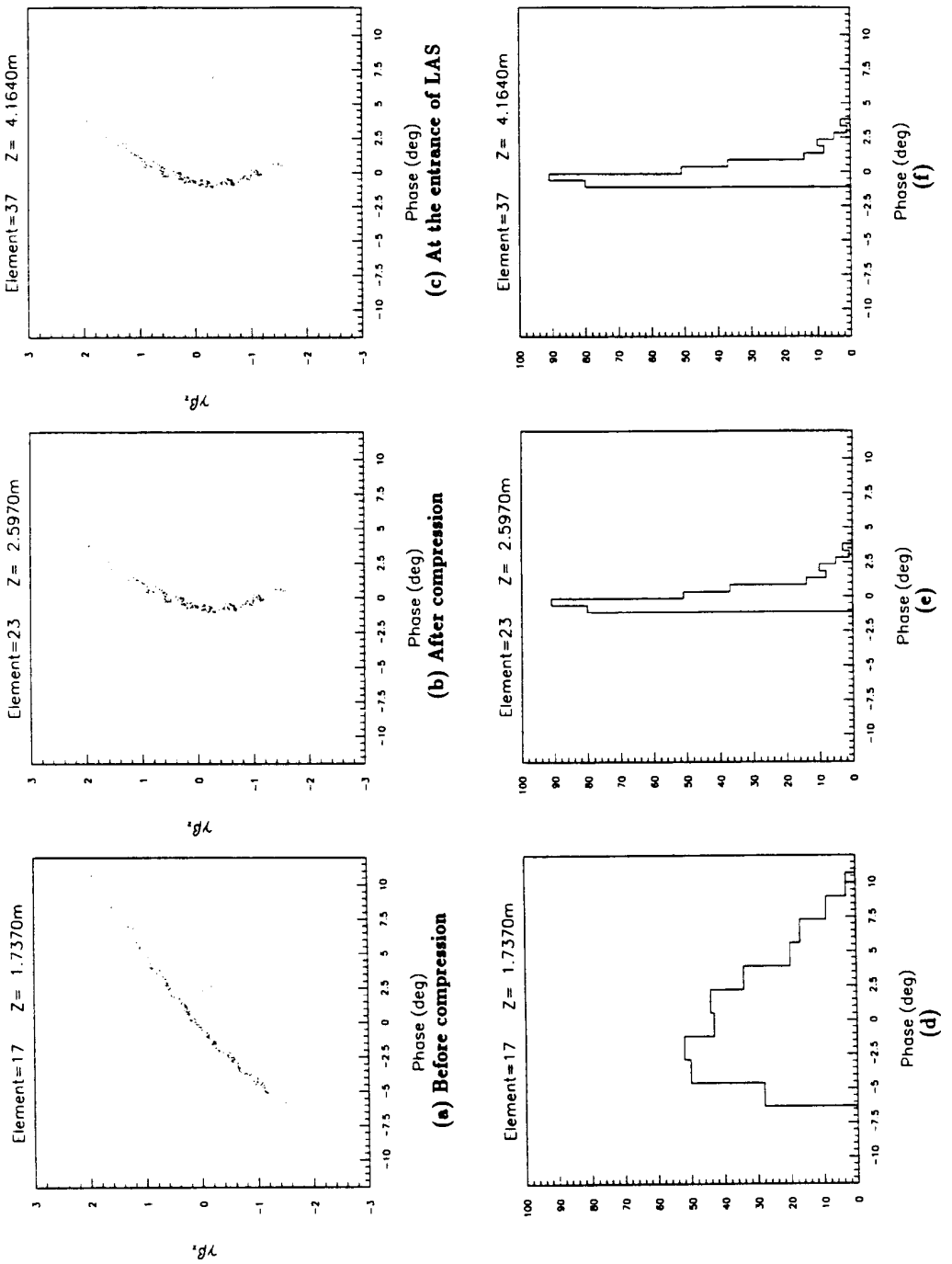

Figure 20: Longitudinal phase space evolution through the CTF line for a 0nC beam.

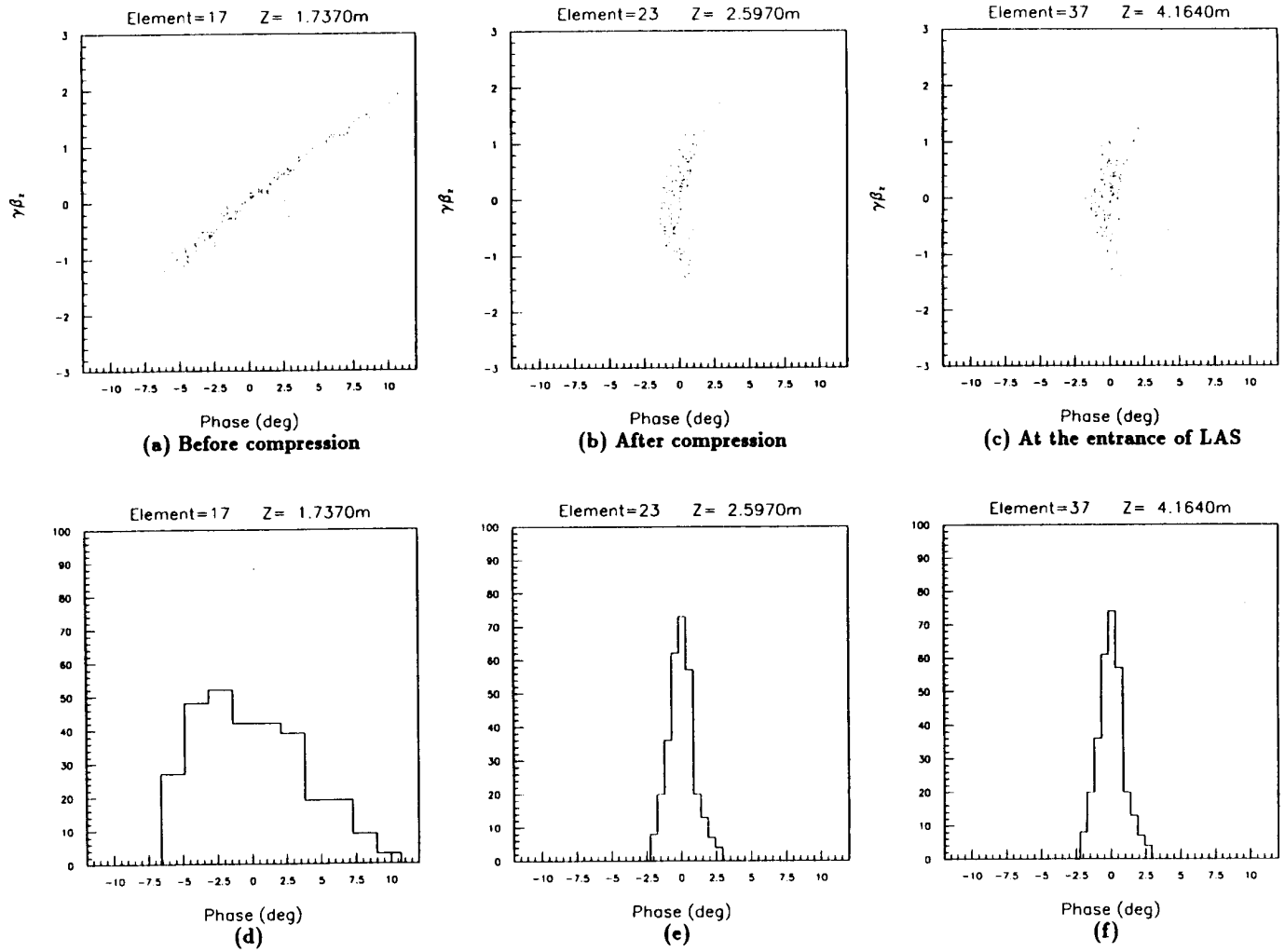

Figure 21: Longitudinal phase space evolution through the CTF line for a 1 nC beam.

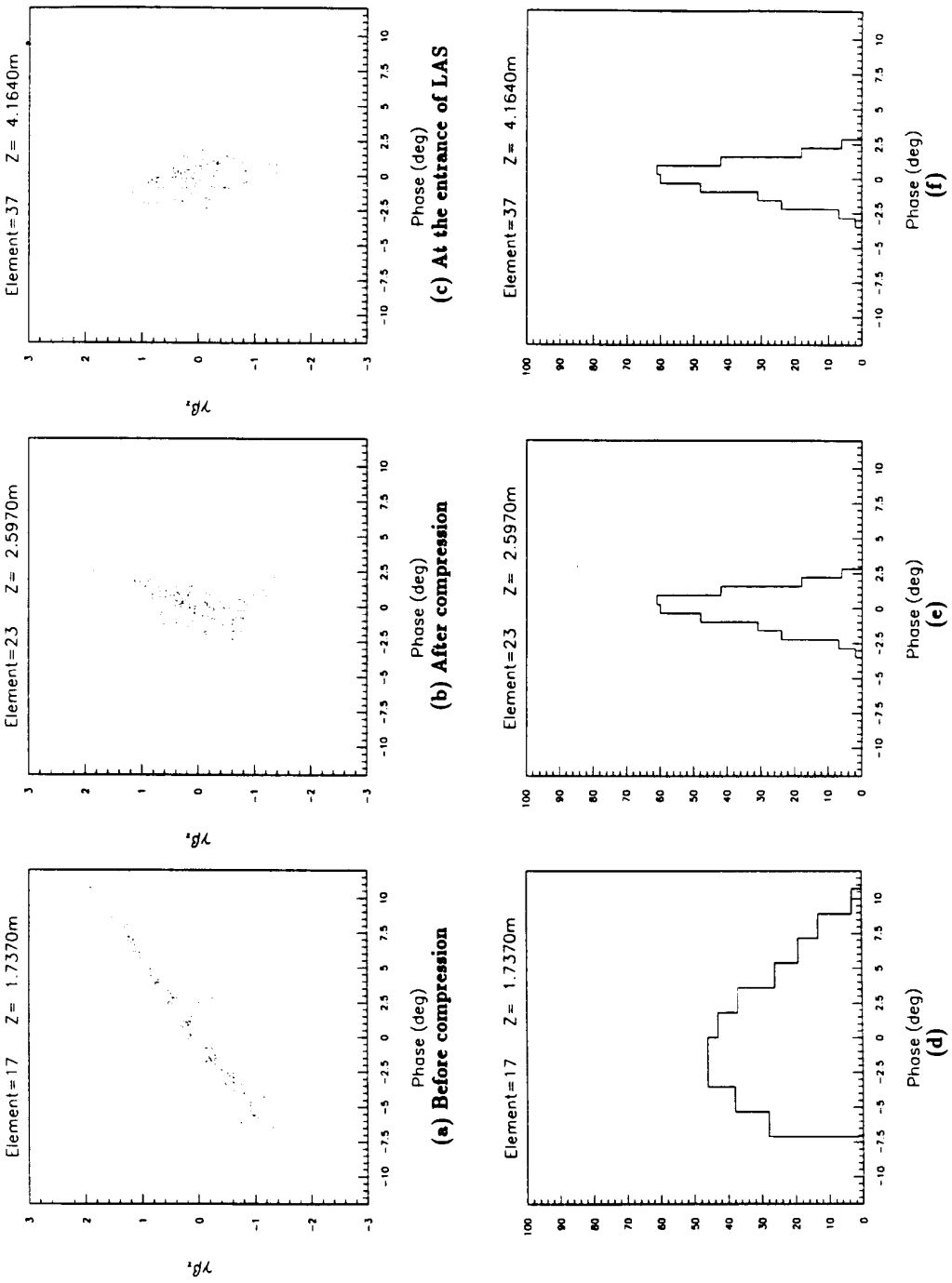

Figure 22: Longitudinal phase space evolution through the CTF line for a 3 nC beam.

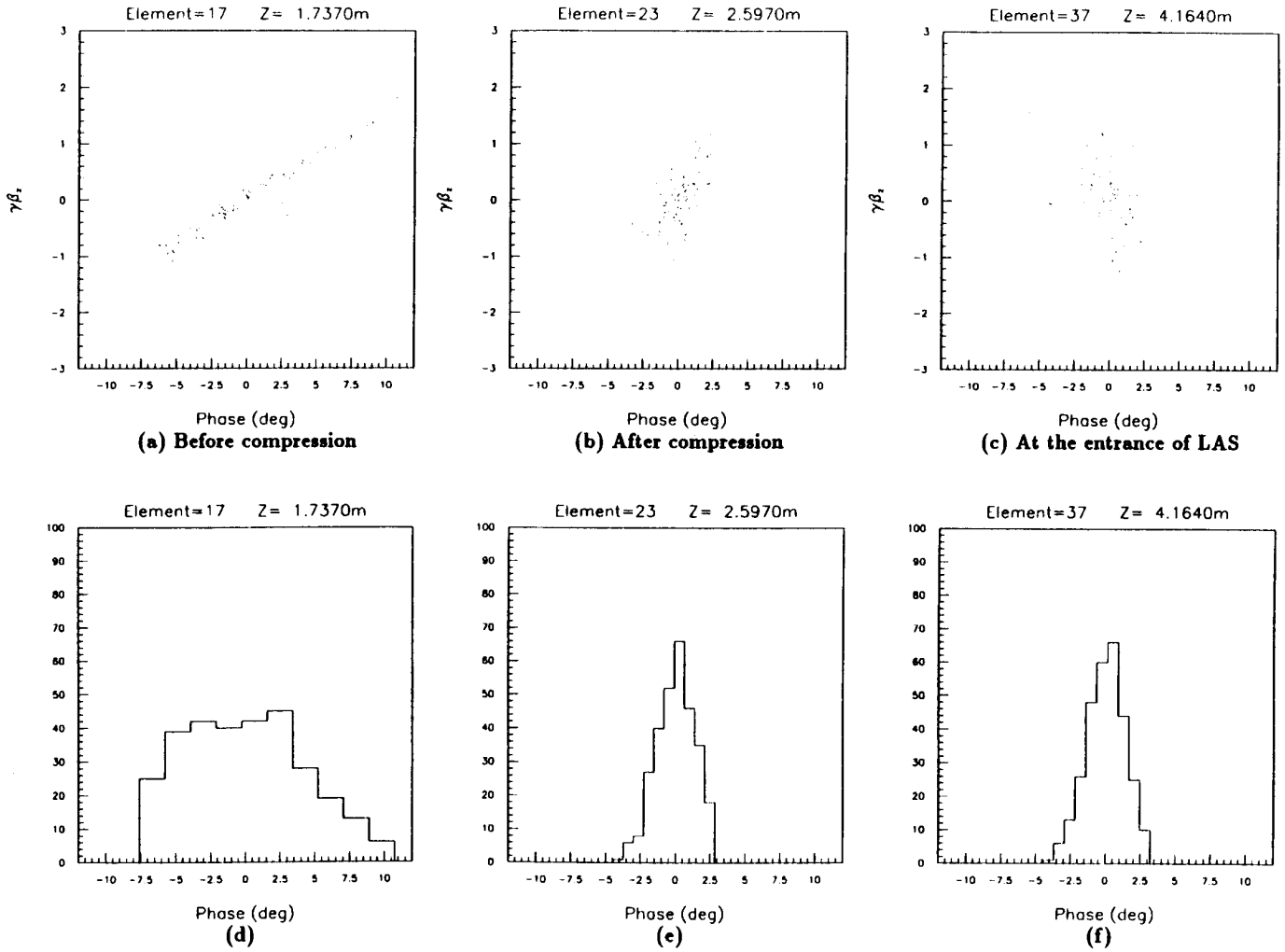

Figure 23: Longitudinal phase space evolution through the CTF line for a 5 nC beam.

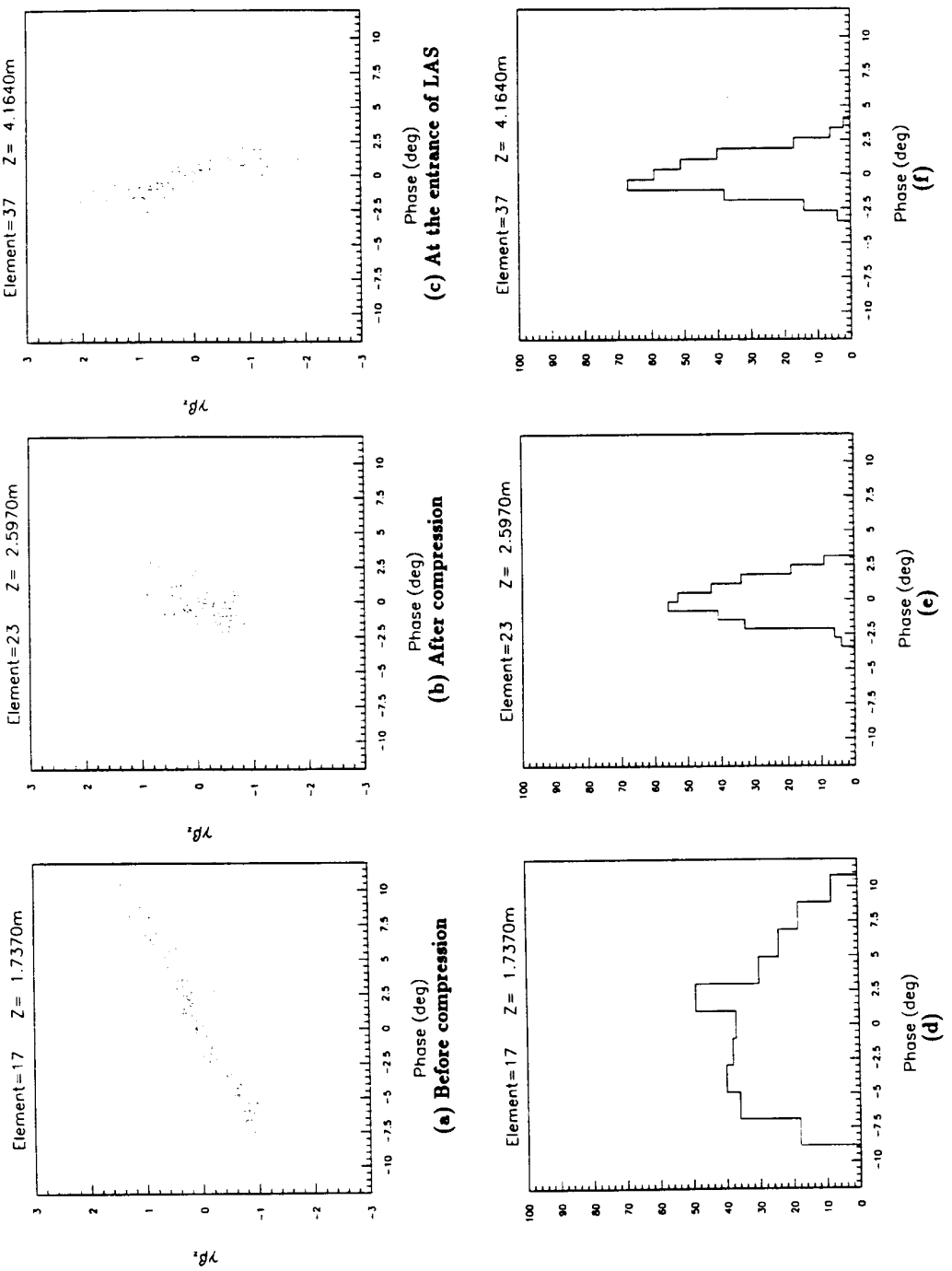

Figure 24: Longitudinal phase space evolution through the CTF line for a 10 nC beam.

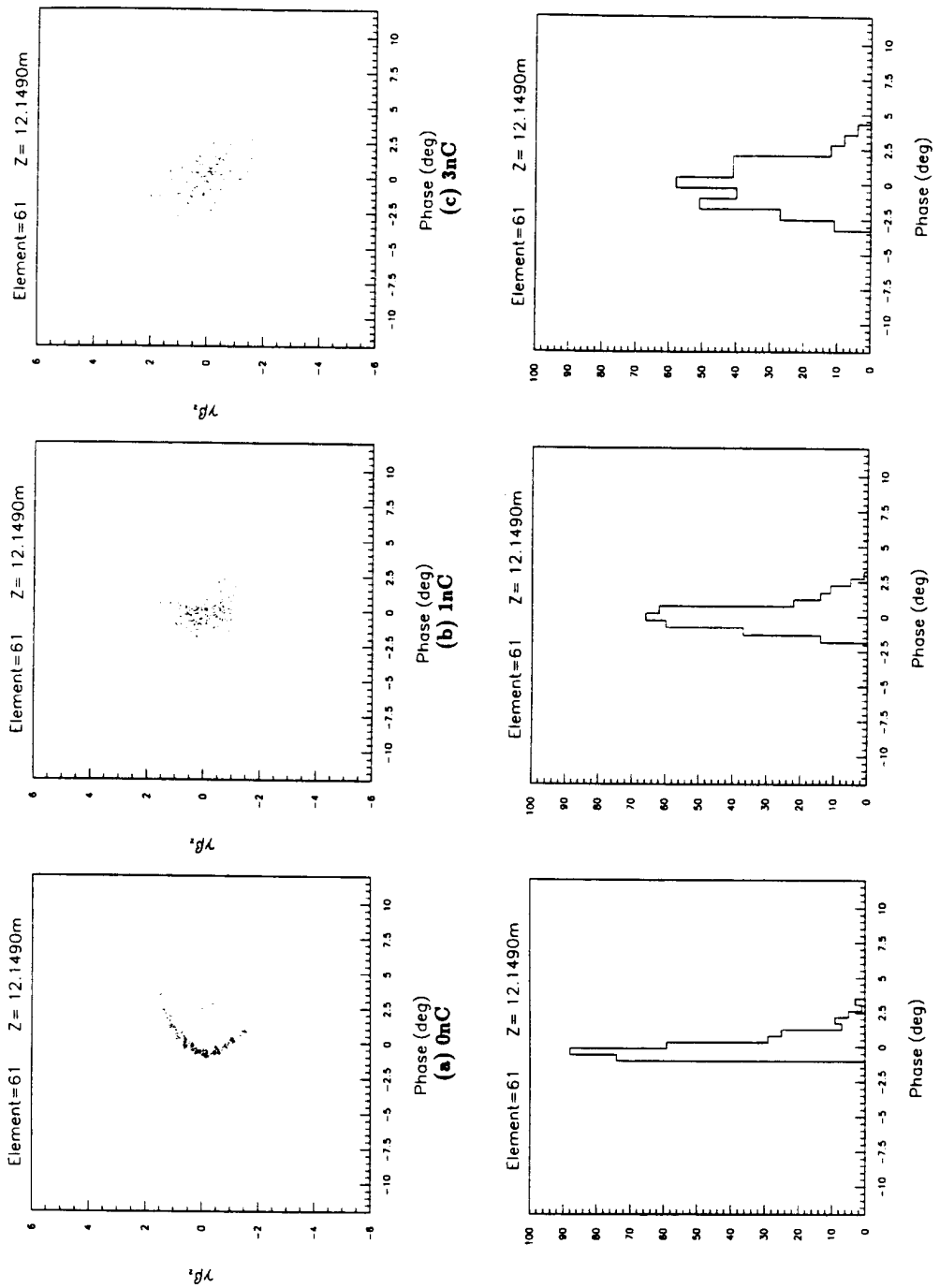

Figure 25: Longitudinal phase space at the TRS (0, 1, 3 nC).

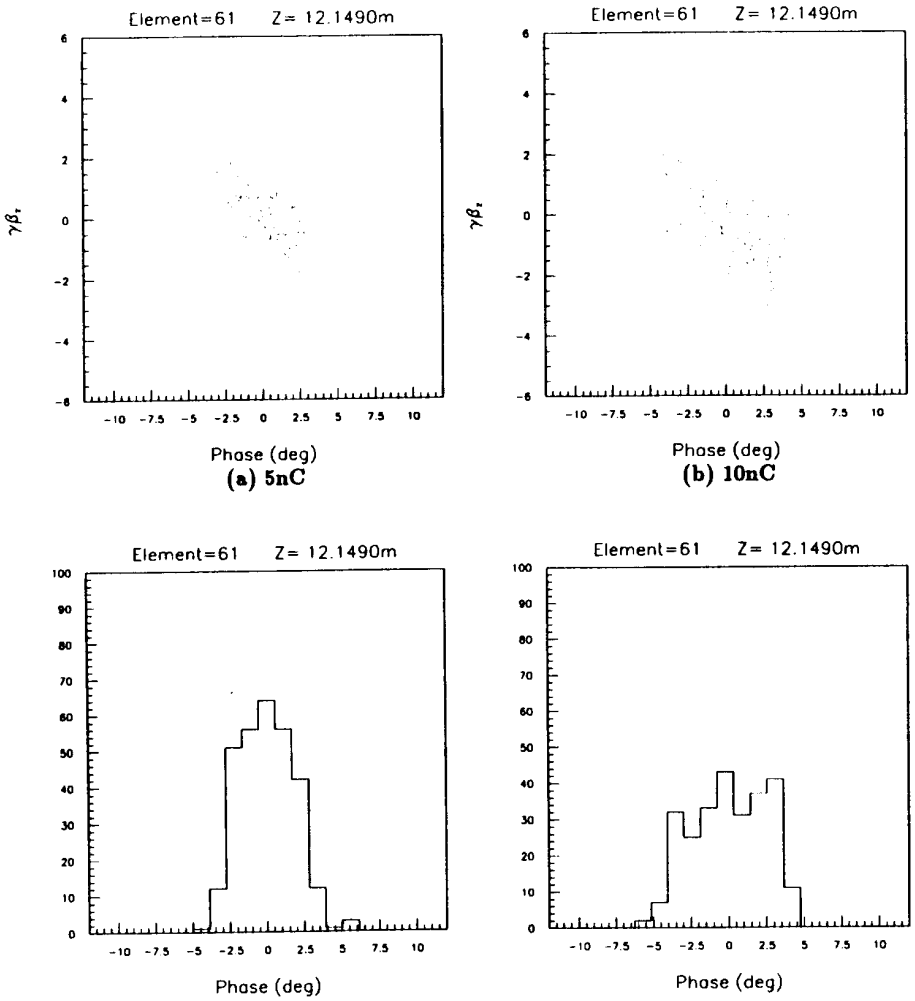

Figure 26: Longitudinal phase space at the TRS (5, 10 nC).

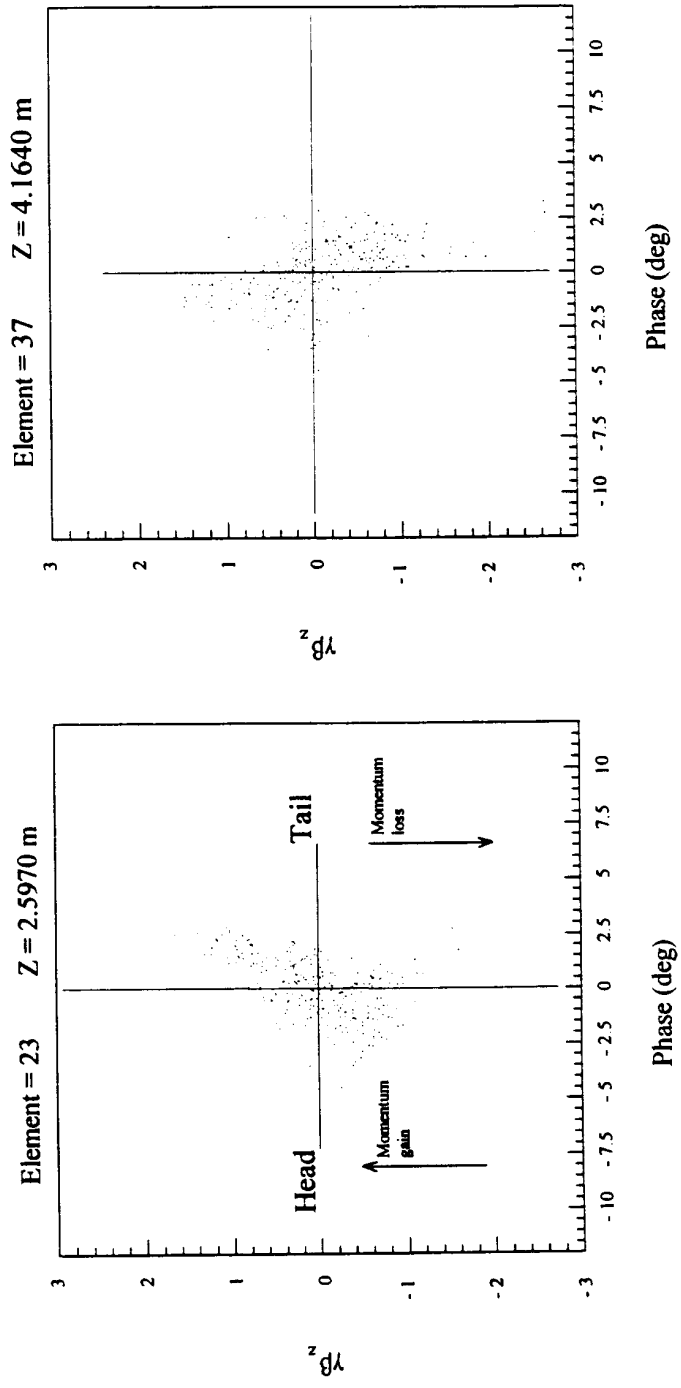

Figure 27: Space charge effect.

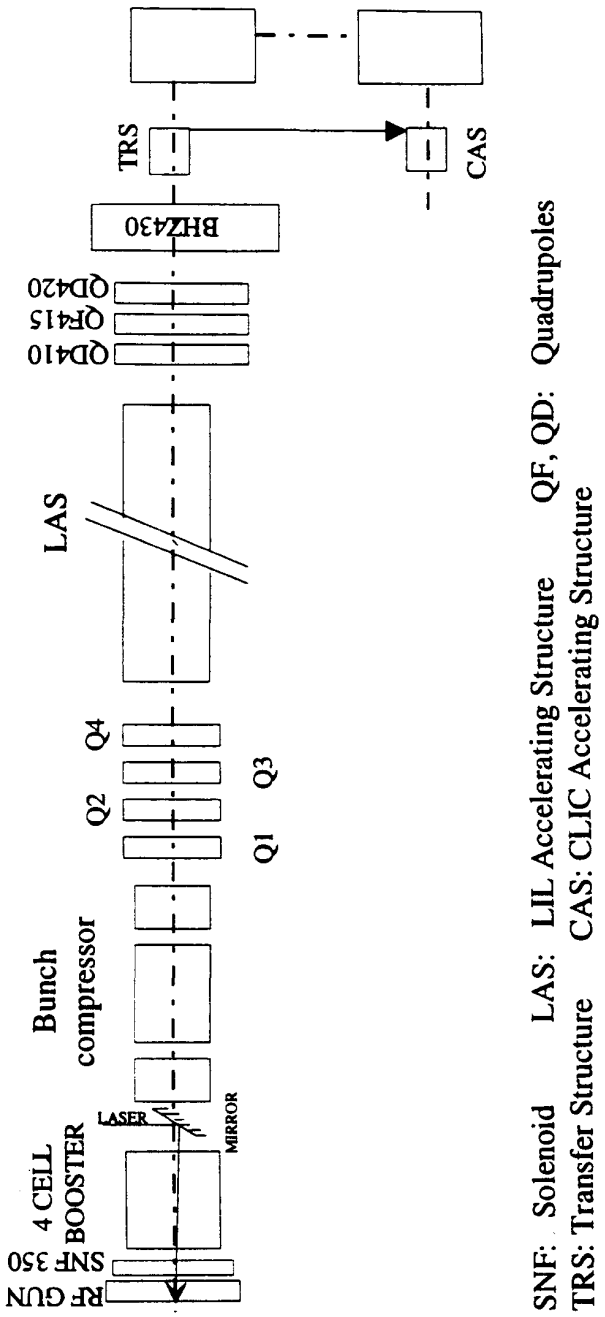

Figure 28: Complete CTF line (1995).

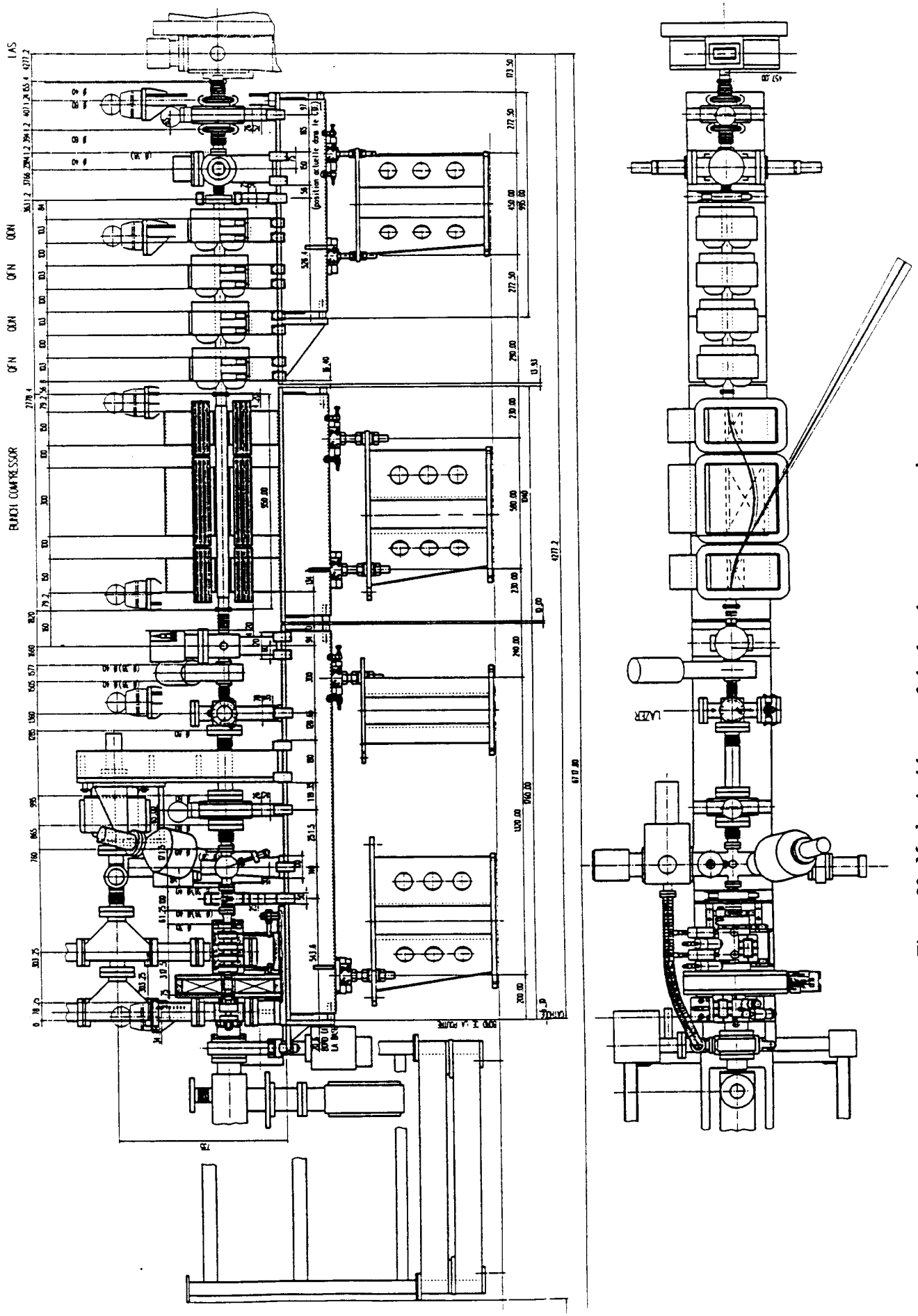

Figure 29: Mechanical layout of the bunch compressor region.

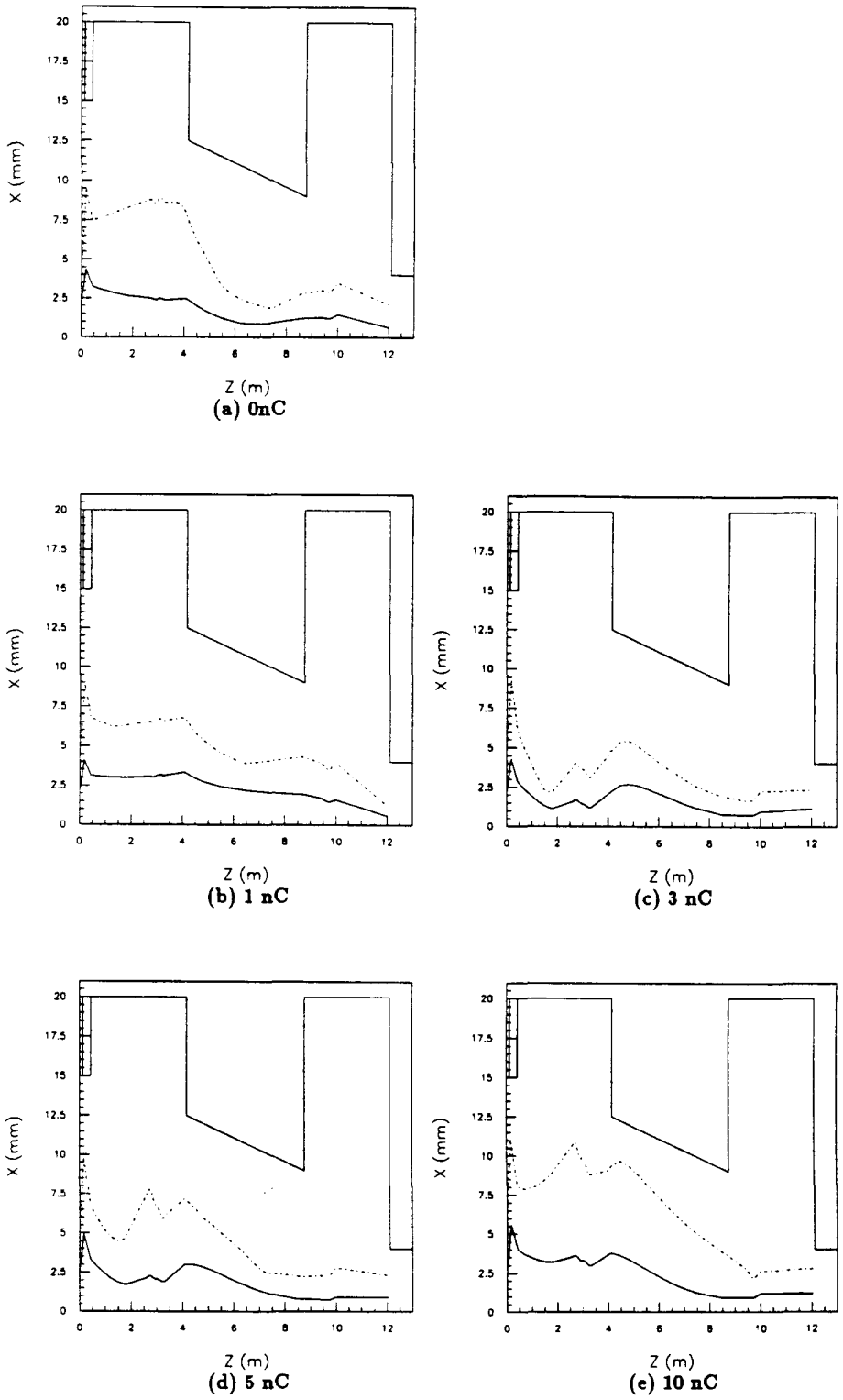

Figure 30: Horizontal beam envelopes with bunch compressor off. (...): 100% particles. (-): rms value.

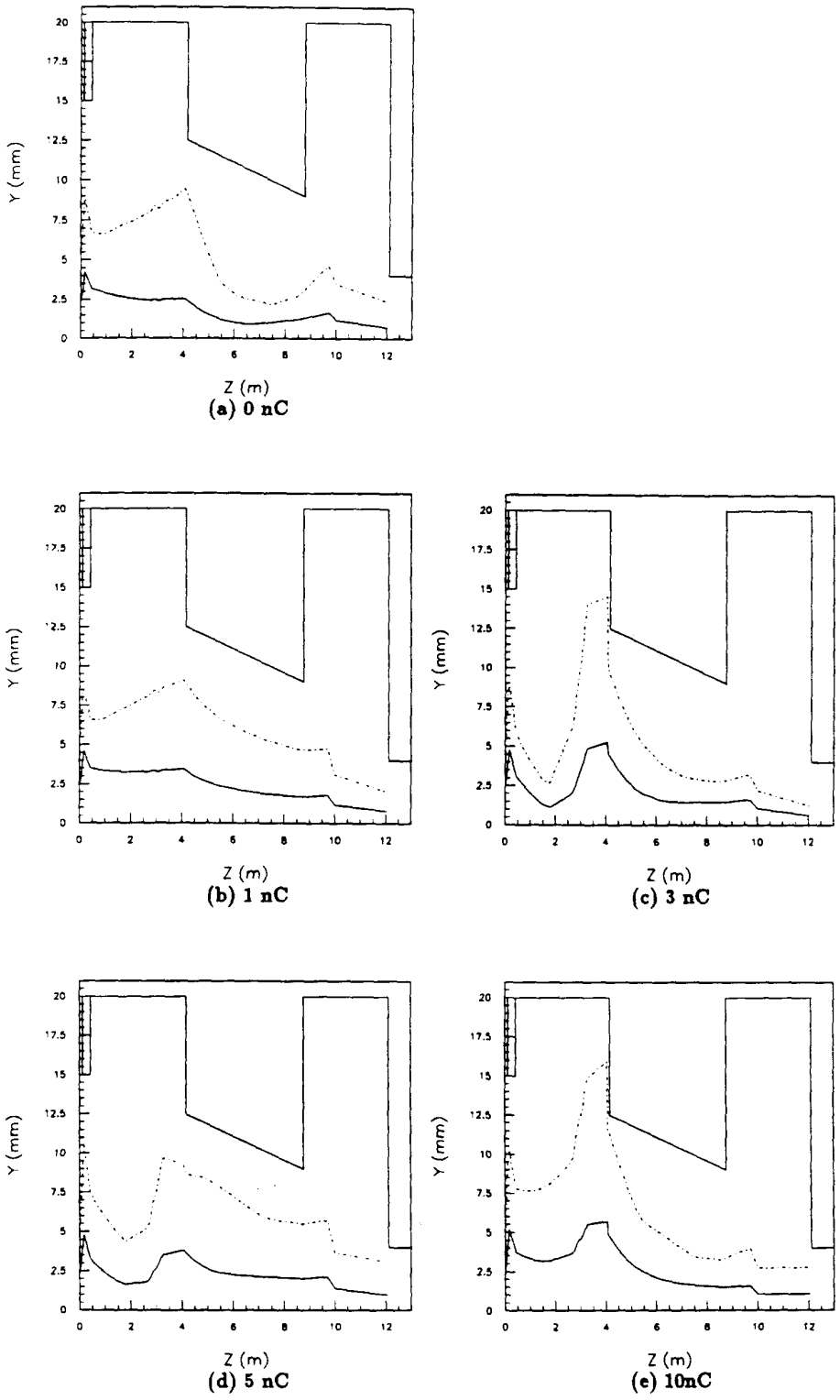

Figure 31: Vertical beam envelopes with bunch compressor off. (...): 100% particles. (-): rms value.

References

[1] J.P. Delahaye. A simplified scheme for 30 GHz RF generation in CTF. *CLIC note 175*

[2] K. Hübner. Generation of 30 GHz power in the CLIC Test Facility. *CLIC note 134*

[3] H. Braun, J.H.B. Madsen and S. Schreiber. The CTF run N ° 4 -1993- Results and comments. *PS/LP/Note 94-07*

[4] J.P. Delahaye, J.H.B. Madsen, A. Riche and L. Rinolfi. Present status and future of the CERN linear collider test facility (CTF). *NIM A340 (1994) 139-145*

[5] E.J.N Wilson. Nonlinear resonances. In *Proceedings of the 1985 CERN Accelerator School, April 1987*

[6] B. Mouton. The PARMELA program (Version 4.3). *LAL/SERA 93-455*

[7] M. Borland. A high-brightness thermionic microwave electron gun. *SLAC-Report-402*

[8] K.L Brown, D.C. Carey, Ch. Iselin and F. Rothacker. Transport. A computer program for designing charged particle beam transport systems. *CERN 80-04*

[9] T.P. Wangler. Introduction to linear accelerators. *Los Alamos Laboratory. LA-UR-93-805*

[10] T.O. Raubenheimer, P. Emma and S. Kheifets. Chicane and wiggler based bunch compressors for futur linear colliders. *SLAC-PUB-6119*

[11] M. Uesaka, T. Kozawa, Y. Yoshida, T. Kobayashi, T. Ueda and K. Miya. Magnetic pulse compression for femto-second single pulse. *Proceedings of the 18th Linear Accelerator Meeting in Japan. Tsukuba. 1993*

[12] S. Kheifets et al. Bunch compression for the TLC: preliminary design. *SLAC-PUB-4802*

[13] R. Corsini. Helical wiggler for bunch compression. *Minutes of the CTF Theory meeting held on 01-07-93*

[14] C.D. Johnson, J. Ströde. An alpha magnet for the CLIC Test Facility. *CERN/PS/LP Note 91-42*

[15] F. Chautard. Minutes of the meeting held on 17 March 1994. *PS/LP/Note 94-12 (Min.)*

[16] P. Marchand, L. Rinolfi. Beam dynamics simulations in the photo-cathode RF gun for the CLIC Test Facility. *Linac Conference 1992, CERN/PS 92-48 (LP), CLIC note 183*

[17] R. Bossart, J.C. Godot, S. Lütgert, A. Riche. Modular RF gun consisting of two RF sections and an intermediate focusing solenoid. *CERN/PS 93-26 (RF), CLIC note 206*